Pekka-Henrik Niemenlehto

Detection of Physiological Events from Biomedical Signals Originating from Facial Landmarks

ACADEMIC DISSERTATION

To be presented, with the permission of the Faculty of Information Sciences of the University of Tampere, for public discussion in the Paavo Koli Auditorium of the University on October 2nd, 2009, at 12 noon.

DEPARTMENT OF COMPUTER SCIENCES
UNIVERSITY OF TAMPERE

A-2009-3
TAMPERE 2009

Supervisor: Professor Martti Juhola, Ph.D.
Department of Computer Sciences
University of Tampere
Finland

Opponent: Docent Alpo Värri, Ph.D.
Department of Signal Processing
Tampere University of Technology
Finland

Reviewers: Professor Tommi Kärkkäinen, Ph.D.
Department of Mathematical Information Technology
University of Jyväskylä
Finland

Assistant Professor Jagdish C. Patra, Ph.D.
School of Computer Engineering
Nanyang Technological University
Singapore

Department of Computer Sciences
FIN-33014 UNIVERSITY OF TAMPERE
Finland

ISBN 978-951-44-7842-0
ISSN 1459-6903

Tampereen yliopistopaino Oy
Tampere 2009

Abstract

This thesis considers the detection of muscle contractions and saccadic eye movements on the basis of biomedical signals originating from facial landmarks. The detection task is performed with detectors that operate on the measured signals and recognise phenomena that are characteristic to the above physiological events. While participating in two successive projects aimed at developing novel human-computer interaction techniques, the author of the thesis designed, implemented, and tested practical detectors that can be used to detect the aforementioned physiological events. The main design goals were the capability of operating in the presence of noise, the capability of adapting to changes in the noise characteristics, the capability of processing signals originating from different subjects without laborious search for suitable parameters, and low computational requirements, which is essential if a detector is used in a near real-time application such as a human-computer interface. The developed detectors can also be used in other types of human-machine interfaces. Example tasks include guiding a wheelchair, operating assistive robots and platforms, and controlling artificial prostheses. Although human-computer interaction gave the basic motivation for the research, there is no reason why the developed detectors could not be used in more traditional medical applications, such as research work, medical diagnosis, and patient monitoring.

Keywords: biomedical signal processing, detection theory, electromyography, electro-oculography.

Acknowledgements

I wish to thank my supervisor Professor Martti Juhola, Ph.D., for his guidance during my postgraduate studies and the preparation of this thesis. I am also grateful to both reviewers, Professor Tommi Kärkkäinen, Ph.D., and Assistant Professor Jagdish C. Patra, Ph.D., for their comments and suggestions. Furthermore, I want to gratefully acknowledge the help I received in different phases of my research from Arto Luoma, Ph.D., Jorma Laurikkala, Ph.D., and Jyrki Rasku, M.Sc. The Department of Computer Sciences has offered a very good work environment, which could not have happened without my wonderful colleagues and capable administration staff. Finally, I want to thank my friends and people close to me for their encouragement and support. Especially, I acknowledge my parents whose support has spanned from my first day at school to the writing of this thesis: mom and dad, I wouldn't have got this far without the two of you.

My studies were funded by (in alphabetical order) Academy of Finland, Alfred Kordelin Trust Fund, Foundation of the University of Tampere, Instrumentarium Science Foundation, and Tampere Graduate School in Information Science and Engineering.

Tampere, June 2009
P.-H. Niemenlehto

Contents

List of Abbreviations

Abbreviation	Description
AC	alternating current
CA	cell-averaging
CDF	cumulative distribution function
CFAR	constant false alarm rate
DC	direct current
DSP	digital signal processing
ECG	electrocardiography
EOG	electro-oculography
EMG	electromyography
FIR	finite impulse response
FAR	false alarm rate
IID	independent and identically distributed
IIR	infinite impulse response
MA	moving average
MLP	multi-layer perceptron
MTPBD	modified two-point backward difference
OS	order-statistic
PDF	probability density function
RMS	root-mean-square
SNR	signal(-of-interest)-to-noise ratio
SOI	signal of interest
TAR	true alarm rate
UMP	uniformly most powerful

List of Original Publications

The thesis is based on the following five publications. In the text they are referred to by their respective Roman numerals.

I. P.-H. Niemenlehto, M. Juhola, and V. Surakka. Detection of electromyographic signals from facial muscles with neural networks. *ACM Transactions on Applied Perception*, Vol. 3, No. 1, January 2006, pp. 48–61.

II. P.-H. Niemenlehto and M. Juhola. Application of a modified two-point backward difference to sequential event detection in surface electromyography. *Journal of Medical Engineering & Technology*, Vol. 33, No. 5, July 2009, pp. 349–360.

III. P.-H. Niemenlehto and M. Juhola. Application of the cell averaging constant false alarm rate technique to saccade detection in electro-oculography. *Proceedings of the 29th Annual International Conference of the IEEE EMBS (EMBC'07)*, pp. 586–589. Institute of Electrical and Electronics Engineers (IEEE), 2007.

IV. P.-H Niemenlehto and M. Juhola. Detection of saccadic eye movements using the order statistic constant false alarm rate technique. *Proceedings of the 6th IASTED International Conference on Biomedical Engineering (BioMED'08)*, pp. 29–33. International Association of Science and Technology for Development (IASTED), 2008.

V. P.-H. Niemenlehto. Constant false alarm rate detection of saccadic eye movements in electro-oculography. *Computer Methods and Programs in Biomedicine*, Vol. 96, 2009, pp. 158–171.

Chapter 1

Introduction

Most organisms belonging to the animal kingdom, including humans, consist of specialised organs that constitute or are parts of various physiological systems. These carry on many vital functions and physiological processes. For example, the circulatory system of a human consists of the heart and the blood vessels. It is responsible for the circulation of the blood and the distribution of oxygen and nutrients in the body. Physiological systems are accompanied by or generate signals that describe their state and functions. Such signals are commonly referred to as biomedical signals, or biosignals for short. Biomedical signals appear in different types, including electrical, acoustic, physical, and biochemical. Most of them can be measured with suitable instruments that range from non-invasive surface electrodes affixed to the skin to invasive catheter-tip sensors inserted into the cardiac chambers of the heart. In this thesis, we are only concerned with biomedical signals that are electrical to begin with. In other words, we are concerned with electrical signals generated by the tissue, the organ, or the physiological system under investigation.

As conveyors of information describing the state and functions of physiological systems, biomedical signals play a significant role in medicine where they are used in research work, medical diagnosis, and patient monitoring. The objective of medical diagnosis is to identify diseases, defects, disorders, damage, or other phenomena adversely affecting the functions and the general well-being of the human body. These phenomena cause alterations in the normal functions of a physiological system and, consequently, alter the signals it generates. Therefore, the analysis of biomedical signals is important when assessing the state of a physiological system. Besides physicians performing medical diagnosis, also paramedics, emergency room staff, and intensive care units make considerable use of biomedical signals in patient monitoring. Novel applications include mobile health monitoring [32, 49, 73]

that can be used to extract information describing the physical condition of the subject. On the basis of this information, it is possible to inform the subject of his or her health status and provide guidelines in daily life as well as in emergency situations. In fact, with this technology it is possible to alert medical personnel to the scene if a medical emergency should occur. This is particularly convenient if the subject is incapacitated and there is no one present who would call the paramedics.

Besides medical work and research, the analysis of biomedical signals has been found valuable in other areas as well. Particularly, the use of biomedical signals in various human-machine interfaces has been investigated. Example tasks include using a traditional computer, guiding a wheelchair, operating assistive robots and platforms, and controlling artificial prostheses. The basic principle is to measure related biomedical signals from the user with suitable instruments, analyse the measured signals in some meaningful manner, and convert them into control commands for the particular machine. As an example, traditional input devices used with computers, such as a keyboard and a mouse, can be replaced with devices based on biomedical signals. The user can, for instance, guide the cursor with his or her gaze and activate objects by contracting facial muscles or execute commands by performing certain facial gestures. Severely disabled people are largely excluded from the benefits of the society. Novel human-machine interfaces enable disabled people to use modern equipment, enjoy more services and benefits, and be an active member of their community. All this probably improves their general quality of life. Although most novel human-machine interfaces are designed for disabled people, new ways to interact with machines may be beneficial for non-handicapped people as well.

None of the applications were possible without suitable signal processing methods. Particularly, the implementation of many applications requires the detection of certain physiological events. Considering the background of the thesis at hand, the need for detectors arose in two successive projects the author participated. The first project, called Wireless Technology and Psychophysiology [89], ran for four years from January 2002 to December 2005. It was funded by the Academy of Finland. The project produced several results, including new wireless measurement devices, models of human physiological measurement, biosignal processing techniques employing wavelets and neural networks, and hands-free multimodal interfaces. The second project, called Face Interface [26], an ideological successor to the first one, started in January 2007 and it is also funded by the Academy of Finland. The aim of the project is to develop a facial prosthesis that can be used to control computers and other electronic devices, such as mobile phones, wirelessly. The prosthesis uses biomedical signals originating from facial musculature and the eyes

measured with novel light weight wireless electrode technology. This new technology will make a significant contribution to the development of user interfaces for people with functional challenges so that many disabilities following from neuronal disorders, such as spinal cord injury or amyotrophic lateral sclerosis, can be attenuated or even overcome. The ultimate goal is to develop a facial prosthesis that is capable of monitoring eye movements and facial muscle activity and, at the very least, mimicking the use of a mouse in a graphical user interface. The second project was still in progress during the writing of this thesis.

This thesis considers the detection of muscle contractions and saccadic eye movements on the basis of biomedical signals originating from facial landmarks. While participating in the two previously mentioned projects, the author of the thesis designed, implemented, and tested practical detectors that can be used to detect the above physiological events. The detection of muscle contractions is performed on the basis of an electromyographic signal that describes the electrical activity of the muscle tissue. The detection of saccadic eye movements is performed by observing the potential changes of an electro-oculographic signal that reflects the movements of the eyes. The main design goals were the capability of operating in the presence of noise, the capability of adapting to changes in the noise characteristics, the capability of processing signals originating from different subjects without laborious search for suitable parameters, and low computational requirements, which is essential if a detector is used in a near real-time application such as the previously envisioned "Face Interface". Because neither medicine nor human-computer interaction but computer science is the major discipline of the author, the research problem has been approached from the technical viewpoints of signal processing and algorithmics. The work and its results are presented in five articles that have been published in refereed international journals and conferences.

The outline of the thesis is as follows. Chapter 2 gives a brief overview of the basics of detection theory, which forms the common foundation for all detection problems. As mentioned above, the work and its results have been presented in form of five articles. These will be summarised in Chapter 3. Also, brief descriptions of the relevant biomedical signals will be given in the same chapter. Finally, we will make some concluding remarks and discuss possible future endeavours in Chapter 4.

Chapter 2

Basic Detection Theory

In many signal processing applications a need arises to determine if a certain type of event occurs at some particular time instant. In practice this is accomplished by passing the observed signal through a particular system, a detector, that makes the decision whether the event has occurred or it has not. The discipline that concentrates on this task is called detection theory, or signal detection theory. The alternative name comes from the fundamental problem of detection theory: we are interested in determining if the observed signal contains a certain signal of interest (SOI) embedded in noise or if the observed signal is composed of noise alone. The SOI is typically understood as a known wave shape, a specific change in the observed signal's characteristics, or some other phenomenon that is associated with the particular event. Much of the early work in detection theory was done in the field of radar research [57, 75, 76]. Besides radar, detection theory has an important role in sonar technology [20], medicine [3, 17, 69, 80], psychophysics [31], various other fields [44], and in numerous mundane appliances, such as automatic fire alarm systems, elevator door sensors, and traffic enforcement cameras. Model change detection, or the detection of abrupt changes [8], can be seen as a sub-discipline of detection theory. Detection theory is also related to pattern recognition [10, 23, 84], where the fundamental problem is to classify a pattern between two or more categories or classes.

2.1 Neyman-Pearson theorem

The foundations of detection theory are in the mathematical and statistical decision theory, where decision making relies on hypothesis testing. In a hypothesis test we are faced with a problem of choosing between two or more competing hypotheses. If we consider the fundamental problem of detection

theory, we have two hypotheses to choose from: either the observed signal is composed entirely of noise or it is a composition of the SOI and noise. The former is referred to as the null hypothesis and the latter is called the alternative hypothesis. Kay [44] defines two primary approaches for simple hypothesis testing: Neyman-Pearson [60] and Bayesian [9]. The method employed depends upon our willingness to incorporate prior knowledge about the probabilities of occurrence of the various hypotheses [44]. If we are able to assign prior probabilities for the hypotheses, we can use the Bayesian approach. However, in most detection problems we cannot say how probable an event is and we have to use the Neyman-Pearson approach instead. Therefore, only the Neyman-Pearson approach will be considered in this discussion. For more information regarding the Bayesian approach, the reader is referred to the literature [9, 10, 23, 44, 84].

Let us denote the null and the alternative hypotheses by H_0 and H_1, respectively. The Neyman-Pearson theorem states that we should decide in favour of H_1 if

$$\Lambda(\mathbf{x}) = \frac{p(\mathbf{x}|H_1)}{p(\mathbf{x}|H_0)} > \gamma, \tag{2.1}$$

where $\Lambda(\mathbf{x})$ is called the likelihood ratio, $\mathbf{x} = [x_0, \ldots, x_{N-1}]$ is an observation vector of N elements, $p(\mathbf{x}|H_0)$ and $p(\mathbf{x}|H_1)$ are the joint probability density functions (PDF) of these N elements under hypotheses H_0 and H_1, respectively, N is a positive integer, and the threshold γ is defined by the probability of false alarm

$$P_{\text{fa}} = \int_{\{\mathbf{x}|\Lambda(\mathbf{x})>\gamma\}} p(\mathbf{x}|H_0)\, d\mathbf{x},$$

which is the probability that the likelihood ratio is larger than the threshold when the observation is composed entirely of noise. The probability of detection

$$P_{\text{d}} = \int_{\{\mathbf{x}|\Lambda(\mathbf{x})>\gamma\}} p(\mathbf{x}|H_1)\, d\mathbf{x}$$

is the probability that the likelihood ratio is larger than the threshold when the observation is a composition of the SOI and noise. Equation (2.1) is known as the likelihood ratio test. This comes from the procedure in which the likelihood ratio is compared with the threshold and the decision between H_0 and H_1 is made accordingly. The Neyman-Pearson theorem states that the likelihood ratio test is optimal in the sense that it maximises P_{d} for a given P_{fa}. A hypothesis test having this property is called a uniformly most powerful (UMP) test. Unfortunately, UMP tests seldom exist and one can exist only if the hypothesis test is one-sided [44].

In hypothesis testing terms, the decision between H_0 and H_1 is made by comparing a relevant test statistic $T(\mathbf{x})$ with a threshold γ'. A decision in favour of H_1 is typically made if

$$T(\mathbf{x}) > \gamma', \tag{2.2}$$

although the direction of the inequality may be the opposite, which depends on the alternative hypothesis. If the hypothesis test is two-sided, both directions have to be taken into consideration. The tests (2.1) and (2.2) appear to be similar. However, the latter is more general because it does not impose limitations on the test statistic. Indeed, the test statistic of a detector is probably dissimilar to the likelihood ratio. Therefore, it is more convenient to define the probabilities of detection and false alarm in terms of the test statistic $T(\mathbf{x})$ and the threshold γ'. By using the simplifying notation $t = T(\mathbf{x})$, we can write

$$P_\mathrm{d} = \int_{\gamma'}^{\infty} f(t|H_1)\, dt \tag{2.3}$$

and

$$P_\mathrm{fa} = \int_{\gamma'}^{\infty} f(t|H_0)\, dt, \tag{2.4}$$

where $f(t|H_1)$ and $f(t|H_0)$ are the test statistic's PDFs under hypotheses H_1 and H_0, respectively. Assuming that all other parameters remain fixed, the choice of the threshold γ' can be seen to have a distinctive effect on the two probabilities. Increasing the threshold in order to decrease P_fa results in a lower P_d, and vice versa. A liberal detector would decide in favour of H_1 every time, which results in $P_\mathrm{d} = P_\mathrm{fa} = 1$. On the other hand, if the detector were conservative, it would decide in favour of H_0 every time, whereupon $P_\mathrm{d} = P_\mathrm{fa} = 0$. All this is to say that unless the detection problem is trivial, false alarms and misses may occur no matter how we choose the threshold. In other words, an undeniable and inevitable truth is that we cannot always be correct whether we wanted to. In realistic situations, uncertainty is always involved when making a decision of any kind. Besides the aforementioned probabilities, two other commonly used measures are the probabilities of miss and correct rejection:

$$P_\mathrm{miss} = 1 - P_\mathrm{d}$$

and

$$P_\mathrm{cr} = 1 - P_\mathrm{fa}.$$

False alarms and misses are also referred to as Type I and II errors, or errors of the first and second kind, respectively.

Example 1 – Change in mean

As an example, let us consider a simple hypothesis testing problem where the elements of $\mathbf{x} = [x_0, \ldots, x_{N-1}]$ are independent and identically distributed (IID) and follow the normal distribution under both the null and the alternative hypothesis:

$$x_k \sim \begin{cases} \mathrm{N}\big(0, \sigma^2\big) & \text{under } H_0 \\ \mathrm{N}\big(\mu, \sigma^2\big) & \text{under } H_1, \end{cases}$$

where both the mean μ and the variance σ^2 are positive and $k = 0, \ldots, N-1$. Because the elements of $\mathbf{x}$ are mutually independent, the likelihood ratio test (2.1) is given by

$$\Lambda(\mathbf{x}) = \frac{\prod_{k=0}^{N-1} \frac{1}{\sigma\sqrt{2\pi}} \exp\left(-\frac{(x_k-\mu)^2}{2\sigma^2}\right)}{\prod_{k=0}^{N-1} \frac{1}{\sigma\sqrt{2\pi}} \exp\left(-\frac{{x_k}^2}{2\sigma^2}\right)} = \frac{\exp\left(-\frac{1}{2\sigma^2}\sum_{k=0}^{N-1}(x_k-\mu)^2\right)}{\exp\left(-\frac{1}{2\sigma^2}\sum_{k=0}^{N-1}{x_k}^2\right)} > \gamma.$$

After taking the natural logarithm of both sides of the inequality and making some simplifications, we get

$$\ln \Lambda(\mathbf{x}) = -\frac{1}{2\sigma^2}\left(-2\mu\sum_{k=0}^{N-1} x_k + N\mu^2\right) > \ln\gamma.$$

This can be further simplified to

$$T(\mathbf{x}) = \frac{1}{N}\sum_{k=0}^{N-1} x_k > \frac{\sigma^2}{N\mu}\ln\gamma + \frac{\mu}{2} = \gamma'.$$

In other words, we should decide in favour of H_1 if the sample mean is sufficiently large. Clearly,

$$T(\mathbf{x}) \sim \begin{cases} \mathrm{N}\big(0, \frac{\sigma^2}{N}\big) & \text{under } H_0 \\ \mathrm{N}\big(\mu, \frac{\sigma^2}{N}\big) & \text{under } H_1. \end{cases}$$

Now, after denoting the mean and the variance of the test statistic under hypothesis H_j by μ_j and ${\sigma_j}^2$ $(j = 0, 1)$, respectively, and recalling (2.3) and (2.4), we get

$$P_\mathrm{d} = \int_{\gamma'}^{\infty} \frac{1}{\sigma_1\sqrt{2\pi}} \exp\left(-\frac{(t-\mu_1)^2}{2{\sigma_1}^2}\right) dt = 1 - \frac{1}{2}\left[1 + \operatorname{erf}\left(\frac{\gamma'-\mu_1}{\sigma_1\sqrt{2}}\right)\right]$$

and

$$P_{\text{fa}} = \int_{\gamma'}^{\infty} \frac{1}{\sigma_0\sqrt{2\pi}} \exp\left(-\frac{(t-\mu_0)^2}{2{\sigma_0}^2}\right) dt = 1 - \frac{1}{2}\left[1 + \text{erf}\left(\frac{\gamma' - \mu_0}{\sigma_0\sqrt{2}}\right)\right],$$

where $\text{erf}(z)$ stands for the error function.[1] One way to choose the threshold value is to set $P_{\text{fa}} = P_{\text{miss}}$ and solve for γ', which yields

$$\gamma' = \frac{\sigma_0\mu_1 + \sigma_1\mu_0}{\sigma_0 + \sigma_1}.$$

The obtained threshold is optimal in the sense that Type I and II errors are equiprobable. One can also fix the false alarm probability and compute the threshold with the inverse cumulative distribution function (CDF) of the normal distribution:

$$\gamma' = \mu_0 + \sigma_0\sqrt{2} \cdot \text{erf}^{-1}\big(2(1 - P_{\text{fa}}) - 1\big).$$

According to the Neyman-Pearson theorem, this threshold maximises P_{d} for the given P_{fa}. Considering the example of Figure 2.1, the first method yields $\gamma' = 1$, whereupon $P_{\text{d}} \approx 0.841$ and $P_{\text{fa}} \approx 0.159$. If the threshold is increased, the P_{fa} is decreased, but so is P_{d}, as discussed earlier. If the inverse CDF method is used instead and it is required, for example, that $P_{\text{fa}} = 0.067$, we get $\gamma' \approx 1.499$ and $P_{\text{d}} \approx 0.692$. ∎

Example 2 – Change in variance

The second example considers a change in variance. Let the elements of $\mathbf{x} = [x_0, \ldots, x_{N-1}]$ be IID and follow $\text{N}(0, {\sigma_0}^2)$ under H_0 and $\text{N}(0, {\sigma_1}^2)$ under H_1. Furthermore, let ${\sigma_1}^2 > {\sigma_0}^2 > 0$. This time the likelihood ratio test (2.1) is given by

$$\Lambda(\mathbf{x}) = \frac{\prod_{k=0}^{N-1} \frac{1}{\sigma_1\sqrt{2\pi}} \exp\left(-\frac{{x_k}^2}{2{\sigma_1}^2}\right)}{\prod_{k=0}^{N-1} \frac{1}{\sigma_0\sqrt{2\pi}} \exp\left(-\frac{{x_k}^2}{2{\sigma_0}^2}\right)} = \frac{\frac{1}{(2\pi{\sigma_1}^2)^{\frac{N}{2}}} \exp\left(-\frac{1}{2{\sigma_1}^2}\sum_{k=0}^{N-1} {x_k}^2\right)}{\frac{1}{(2\pi{\sigma_0}^2)^{\frac{N}{2}}} \exp\left(-\frac{1}{2{\sigma_0}^2}\sum_{k=0}^{N-1} {x_k}^2\right)} > \gamma.$$

[1] The error function

$$\text{erf}(z) = \frac{2}{\sqrt{\pi}} \int_0^z \exp\left(-t^2\right) dt$$

is encountered when evaluating the CDF of the normal distribution. It is an odd function and has an inverse function such that

$$\text{erf}\left(\text{erf}^{-1}(z)\right) = \text{erf}^{-1}\left(\text{erf}(z)\right) = z.$$

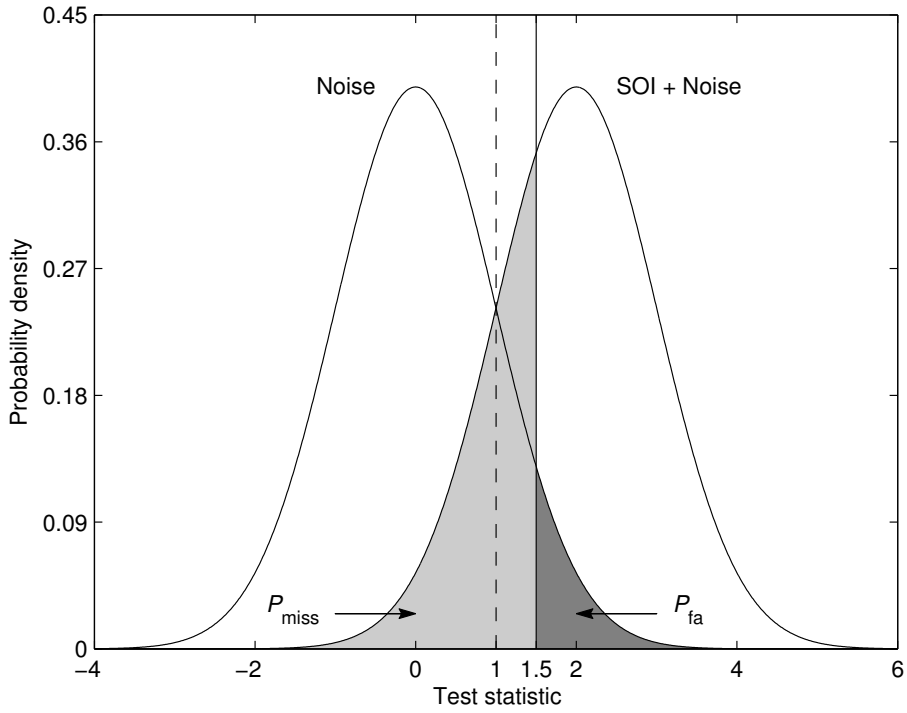

Figure 2.1: Test statistic's PDFs in a simple hypothesis testing problem. If the observation consists only of noise, $T(\mathbf{x}) \sim \mathrm{N}(0,1)$, but if the SOI is present, $T(\mathbf{x}) \sim \mathrm{N}(2,1)$. The vertical dashed and solid lines correspond to thresholds $\gamma' = 1$ and $\gamma' = 1.5$, respectively. If $\gamma' = 1$, $P_\mathrm{d} = P_\mathrm{cr} \approx 0.841$ and $P_\mathrm{fa} = P_\mathrm{miss} \approx 0.159$. On the other hand, if $\gamma' = 1.5$, $P_\mathrm{d} \approx 0.691$, $P_\mathrm{cr} \approx 0.933$, $P_\mathrm{fa} \approx 0.067$, and $P_\mathrm{miss} \approx 0.309$. The latter two have been highlighted as dark grey and light grey areas.

After taking the natural logarithm of both sides of the inequality and making some simplifications, we get

$$\ln \Lambda(\mathbf{x}) = \frac{N}{2} \ln \left(\frac{{\sigma_0}^2}{{\sigma_1}^2} \right) - \frac{1}{2} \left(\frac{1}{{\sigma_1}^2} - \frac{1}{{\sigma_0}^2} \right) \sum_{k=0}^{N-1} {x_k}^2 > \ln \gamma,$$

which can be further simplified to

$$T(\mathbf{x}) = \frac{1}{N} \sum_{k=0}^{N-1} {x_k}^2 > \frac{\frac{2}{N} \ln \gamma - \ln \left(\frac{{\sigma_0}^2}{{\sigma_1}^2} \right)}{\frac{1}{{\sigma_0}^2} - \frac{1}{{\sigma_1}^2}} = \gamma'.$$

That is to say, we should decide in favour of H_1 if the sample variance is

large enough. Because the test statistic is a scaled version of a chi-square distributed random variable, it follows the gamma distribution under both hypotheses [53]:

$$T(\mathbf{x}) \sim \begin{cases} \Gamma\left(\frac{N}{2}, \frac{2{\sigma_0}^2}{N}\right) & \text{under } H_0 \\ \Gamma\left(\frac{N}{2}, \frac{2{\sigma_1}^2}{N}\right) & \text{under } H_1. \end{cases} \tag{2.5}$$

An intuitive approach would be to choose

$$\gamma' = \frac{{\sigma_0}^2 + {\sigma_1}^2}{2}.$$

But then again, an optimal threshold value in the Neyman-Pearson sense can be computed with the inverse CDF of the gamma distribution. For example, let $N = 10$, ${\sigma_0}^2 = 1$, and ${\sigma_1}^2 = 3.5$. By using our intuitive approach, we get $\gamma' = 2.25$, $P_\mathrm{d} \approx 0.778$, and $P_\mathrm{fa} \approx 0.013$. But if we use the inverse CDF method instead and require, for example, that $P_\mathrm{fa} = 10^{-2}$, we get $\gamma' \approx 2.321$ and $P_\mathrm{d} \approx 0.760$. ■

The preceding discussion addressed the simple hypothesis testing problem, where it is assumed that the PDF of the observation is completely known under each hypothesis. Particularly, it is assumed that both the distribution families and respective distribution parameters are completely known. This is necessary if we want to construct the likelihood ratio test: the likelihood ratio in (2.1) depends on the PDF of the observation under both hypotheses. In certain situations, we can make assumptions regarding the distribution families, but we do not necessarily know all parameters. For example, even though we do not have a complete knowledge of the interference, in most situations it is assumed to be additive white Gaussian noise of zero mean. The Gaussian noise assumption is done for mathematical simplicity and it is usually justified by the central limit theorem: the superposition of numerous noise sources should be approximately normally distributed. If we have only limited knowledge of the distribution parameters, we are faced with the composite hypothesis testing problem. The unknown parameters can be replaced with their maximum likelihood estimates, which leads to the generalised likelihood ratio test [44]. Also other factors, such as the complexity of the likelihood ratio or statistical dependency, may complicate the Neyman-Pearson approach. The aforementioned issues do not necessarily foil the design process if some other approach is used. Indeed, the design of a detector seldom begins analytically, but instead by making observations of the SOI and the inherent noise. Based on these observations, we attempt to design a suitable detector that does not necessarily have much in common with the Neyman-Pearson approach. The detector is then evaluated and re-

designed if it fails to operate satisfactorily. Most often experience, and even intuitiveness, contributes to the design of a detector.

2.2 Practical detectors

A considerable number of signal processing applications function in real-time, or more precisely in near real-time, whereupon practical detectors have to be able to operate on sequential data. Because most signal processing is nowadays carried out with digital signal processing (DSP) techniques [22, 37, 59, 62, 77], it is convenient to comprehend detectors as discrete-time systems. The input of a discrete-time system is a signal that is represented by a sequence

$$x(n) = x_{\mathrm{c}}(nT_{\mathrm{s}}),$$

where $x_{\mathrm{c}}(nT_{\mathrm{s}})$ is the analogue continuous-time signal that is sampled in order to produce the discrete-time signal $x(n)$, the time index n is an integer, and the constant T_{s} is the sampling interval in seconds, which is the reciprocal of the sampling frequency

$$F_{\mathrm{s}} = 1/T_{\mathrm{s}} \quad (\mathrm{Hz} = \mathrm{s}^{-1}).$$

According to the Nyquist-Shannon sampling theorem, the sampling frequency has to be at least twice the bandwidth of the continuous-time signal for the samples to describe it completely.[2]

A generic discrete-time detector can be understood as a cascade of two sub-units, as portrayed in Figure 2.2. On the basis of the input signal $x(n)$, the test function computes the test statistic $T(n)$. It serves as an input to the decision logic that makes the decision regarding the presence of the SOI. Typically, the decision logic performs a simple comparison and decides in favour of H_1 if

$$T(n) > \gamma'.$$

The above test is almost identical to the test (2.2), the only difference being the notation. Particularly, the test statistic is not a function of the observation vector $\mathbf{x}$, but a function of the time index n. However, the observation

[2]The sampling theorem is named for Harry Nyquist and Claude Shannon. It was introduced by Nyquist [61] in 1928 and proved by Shannon [74] in 1949. The sampling theorem states that a continuous-time signal has to be bandlimited below the Nyquist frequency, which is half of the sampling frequency, before sampling. If this condition is not achieved, the higher frequencies are aliased so that the original signal cannot be unambiguously constructed from its sampled representation.

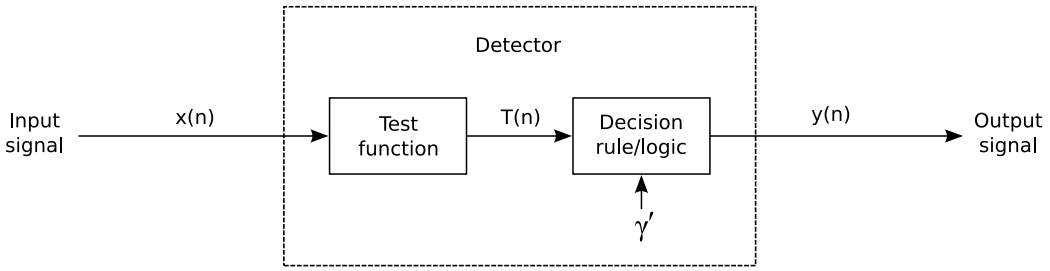

Figure 2.2: Block diagram of a generic discrete-time detector.

vector can be understood as a snapshot in time so that its elements correspond to consecutive samples of the input signal. The analogy can be expressed with the identity

$$x_k = x(n-k), \tag{2.6}$$

where $k = 0, \ldots, N-1$. The outcome of the test is reflected by the binary output signal

$$y(n) = \begin{cases} 1 & \text{if } T(n) > \gamma' \\ 0 & \text{otherwise.} \end{cases}$$

The decision logic may be more sophisticated if necessary. For example, it may involve the estimation of several SOI related parameters that are used in conjunction with the test statistic to make the final decision. Indeed, several unambiguous criteria may have to be fulfilled before a decision in favour of H_1 is made.

It depends mainly on the requirements of the framework system whether the output signal should be one for each time step the detection criteria are fulfilled. If the task is to detect the discrete occurrences of the SOI, then it is convenient that the detector gives an indication of detection only once for each detected occurrence. This may happen, for example, after all criteria have been fulfilled. New detections are typically impossible until a certain refraction criterion has been fulfilled. For example, it may be required that the test statistic has to cross the threshold in the opposing direction before new detections are possible. In addition, premature detections are typically suppressed by preventing the decision logic from making any decisions until the detector is fully immersed in the input signal. This can be accomplished, for example, by fixing the test statistic to some neutral value until full immersion occurs. Naturally, the exact immersion requirements depend on the actual implementation.

Because practical detectors operate on sequential data, the input samples contributing to the test statistic will occasionally originate from a region that

can be understood as a transition between H_0 and H_1. Therefore, it is justified to ask are the probabilities of detection and false alarm valid measures of detection performance. They are because it does not make much of a difference whether detection is triggered by data that completely consists of the SOI or only partially does. It is usually assumed that if detection had occurred in the latter case, then it would certainly have happened in the former case as well. By making such assumption, one simplifies the performance evaluation of a detector. Therefore, when evaluating the detection performance of a detector, it is customary to consider only H_0 and H_1 and to omit transitional hypotheses.

Example 3 – Segment boundary detection

In certain applications it may be necessary to identify boundaries between signal segments that reflect different states of nature. From the viewpoint of detection theory, the problem is to detect changes in the observed signal that can be perceived as indicators of segment boundaries. In other words, a specific change makes up the SOI. This example considers a simple model change detection problem. For a more in-depth treatment, the reader is referred to [8] and [44]. Let

$$x(n) \sim \mathrm{N}\big(0, \sigma^2\big) \quad \text{under } H_0$$

and

$$x(n) \sim \begin{cases} \mathrm{N}\big(0, {\sigma_0}^2\big) & \text{before change} \\ \mathrm{N}\big(0, {\sigma_1}^2\big) & \text{after change} \end{cases}$$

under H_1, where σ^2, ${\sigma_0}^2$, and ${\sigma_1}^2$ are positive and ${\sigma_0}^2 \neq {\sigma_1}^2$. The detection problem is similar to the one considered in Example 2, albeit there are two differences. First, the hypothesis test is two-sided. Second, we do not only want to determine that a change has occurred, but we also want to determine when it occurred. We will consider a detector that is shown in Figure 2.3. The test statistic is computed with a cascade of a square-law rectifier, an N-point moving average (MA) filter, and a division operator. The output of the MA filter is an estimate of the signal variance. Because of the N-point delay line, the numerator and the denominator of the division correspond to adjacent regions of the input signal. The detector implements the famous Fisher's F-test for the equality of variances:

$$T(n) = \frac{\dfrac{1}{N}\displaystyle\sum_{k=0}^{N-1} x^2(n-k)}{\dfrac{1}{N}\displaystyle\sum_{k=N}^{2N-1} x^2(n-k)} > \gamma' \quad \text{or} \quad T(n) < {\gamma'}^{-1}.$$

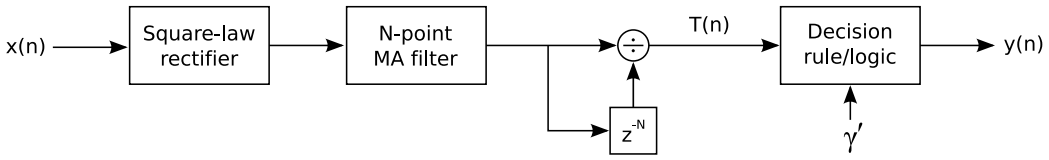

Figure 2.3: Block diagram of a detector that can be used to locate a change in the variance of a zero mean signal. This detector implements Fisher's F-test for the equality of variances.

In other words, we decide in favour of H_1 if either of the inequalities holds. Clearly,

$$T(n) \sim \mathrm{F}\big(N, N\big) \quad \text{under } H_0$$

and

$$P_{\mathrm{fa}} = F_{N,N}\big(\gamma'^{-1}\big) + 1 - F_{N,N}\big(\gamma'\big),$$

where $F_{d_1,d_2}(z)$ stands for the CDF of the F-distribution with d_1 numerator and d_2 denominator degrees of freedom. A detector whose test statistic's PDF does not depend on the noise variance under H_0 is called a constant false alarm rate (CFAR) detector [44, 75, 76]. Because this is the case, the considered detector is a CFAR detector. The main advantage of a CFAR detector is that the threshold can be determined without knowledge of the noise variance. Indeed, a threshold value that guarantees a desired P_{fa} can be computed with the inverse CDF method:

$$\gamma' = F_{N,N}^{-1}\left(1 - \frac{P_{\mathrm{fa}}}{2}\right).^{3}$$

According to our earlier discussion regarding transitional hypotheses, we define that under H_1 the segment boundary coincides with the time index $n - N + 0.5$, which is located between the signal regions contributing to the numerator and the denominator of the test statistic. The test statistic deviates from unity according to the variance ratio ${\sigma_1}^2/{\sigma_0}^2$ under H_1. Hence,

$$\frac{{\sigma_0}^2}{{\sigma_1}^2} \cdot T(n) \sim \mathrm{F}\big(N, N\big) \quad \text{under } H_1.$$

[3] We have used the property

$$F_{d,d}(z^{-1}) = 1 - F_{d,d}(z),$$

which follows from the properties of the regularised incomplete beta function that is used to define the CDF of the F-distribution.

When determining P_d, one has to take into account the two-sided nature of the hypothesis test and consider the two possible change directions separately:

$$P_\mathrm{d} = \begin{cases} 1 - F_{N,N}\left(\frac{{\sigma_0}^2}{{\sigma_1}^2} \cdot \gamma'\right) & \text{if } {\sigma_1}^2 > {\sigma_0}^2 \\ F_{N,N}\left(\frac{{\sigma_0}^2}{{\sigma_1}^2} \cdot \gamma'^{-1}\right) & \text{if } {\sigma_0}^2 > {\sigma_1}^2. \end{cases}$$

The detector gives an indication of a segment boundary only once for each detection. New detections are impossible until the corresponding threshold is crossed again in the opposite direction. An estimate of the segment boundary location is computed by subtracting $N - 0.5$ samples from the location of the local extremum that is found between the threshold crossings. This places the estimate between the aforementioned signal regions. The first $2N - 1$ values of the test statistic are fixed to unity in order to guarantee the suppression of premature detections.

An application example is shown in Figure 2.4. The objective was to detect segment boundaries where the signal variance changed by a significant amount. A white Gaussian noise signal with zero mean and unity variance was amplitude modulated with an envelope waveform whose amplitude was switched between 1 and 2, whereupon the variance ratio can theoretically reach 4 or 0.25 at a segment boundary, depending on the direction of the change. The sampling frequency was 1 kHz. The length of the MA filter was 201 samples, whereupon the first 401 values of the test statistic were fixed to unity in order to prevent premature detections. The threshold $\gamma' \approx 2.009$ was computed with the inverse CDF method for $P_\mathrm{fa} = 10^{-6}$. It yields $P_\mathrm{d} \approx 1$ for both directions. ■

Example 4 – Matched filtering

If the SOI is a deterministic signal, it is possible to use a well-known technique called matched filtering [17, 31, 37, 44, 69, 76, 77]. A matched filter is a linear filter whose impulse response is the time inverse of the SOI, or its close approximation. The matched filter is optimal in the sense that it maximises the signal(-of-interest)-to-noise ratio (SNR) at its output. The matched filter can be derived in different ways. In this example we will use the Neyman-Pearson approach. Let

$$x(n-k) = \begin{cases} w(n-k) & \text{under } H_0 \\ h(k) + w(n-k) & \text{under } H_1 \end{cases},$$

where the noise samples $w(n-k)$ are IID and follow $\mathrm{N}(0, \sigma^2)$ with $\sigma^2 > 0$, $h(k)$ is the N-point impulse response of the matched filter, and $k = 0, \ldots, N-1$.

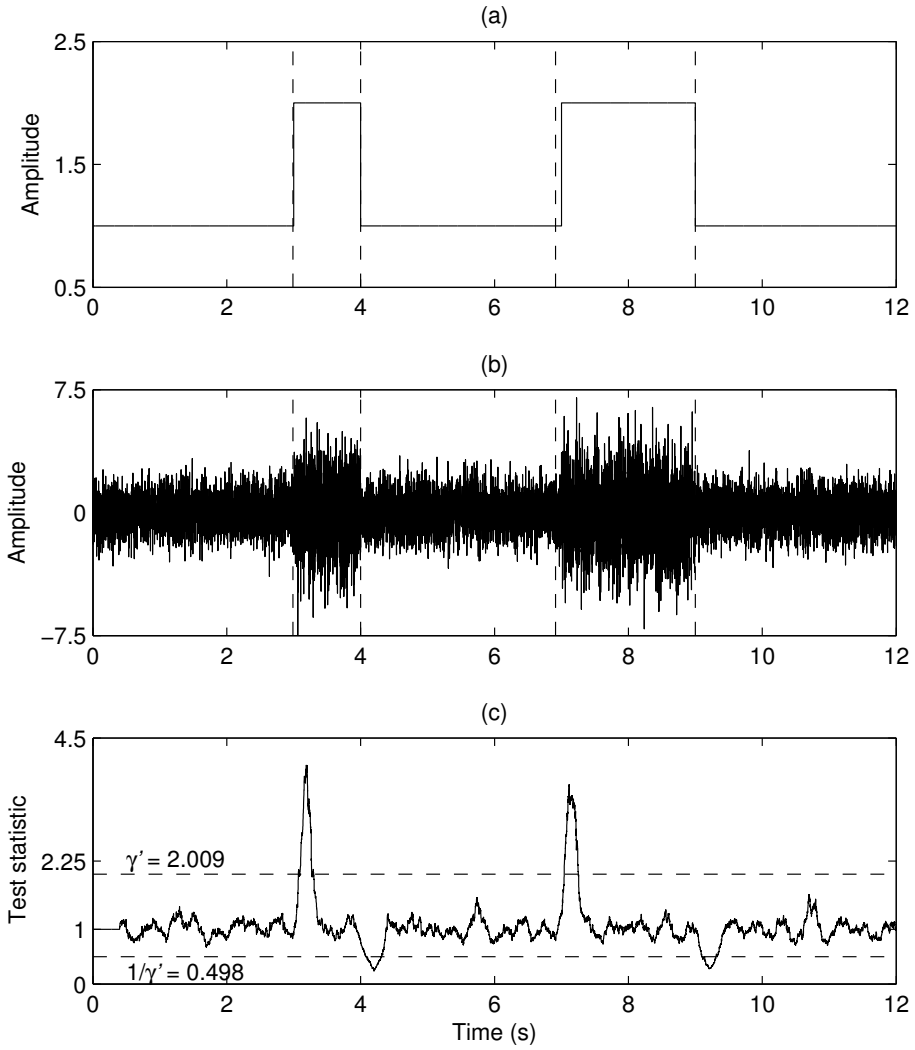

Figure 2.4: Example of using the detector of Figure 2.3 to detect segment boundaries defined by the envelope waveform (a) from a noisy signal (b). The vertical dashed lines represent location estimates of the detected segment boundaries. The test statistic (c) represents the variance ratio between adjacent signal regions. The horizontal dashed lines represent a two-sided threshold chosen to accommodate for $P_{\text{fa}} = 10^{-6}$.

By using the notational identity (2.6), the likelihood ratio (2.1) can be written as follows:

$$\Lambda(\mathbf{x}) = \frac{\prod_{k=0}^{N-1} \frac{1}{\sigma\sqrt{2\pi}} \exp\left(-\frac{\big(x(n-k)-h(k)\big)^2}{2\sigma^2}\right)}{\prod_{k=0}^{N-1} \frac{1}{\sigma\sqrt{2\pi}} \exp\left(-\frac{x^2(n-k)}{2\sigma^2}\right)} > \gamma.$$

After applying the identities of exponentiation, taking the natural logarithm of both sides of the inequality, and making simplifications, the above test can be expressed as

$$\ln\Lambda(\mathbf{x}) = -\frac{1}{2\sigma^2}\left(-2\sum_{k=0}^{N-1} h(k)x(n-k) + \underbrace{\sum_{k=0}^{N-1} h^2(k)}_{\varepsilon}\right) > \ln\gamma.$$

This can be further simplified to

$$T_0(n) = \sum_{k=0}^{N-1} h(k)x(n-k) > \sigma^2\ln\gamma - \frac{\varepsilon}{2} = \gamma_0',$$

where ε is the squared sum of the impulse response. The test statistic is the convolution between the matched filter's impulse response and the input signal, which is essentially what is done when a signal is filtered with a discrete-time filter. One can show that

$$T_0(n) \sim \begin{cases} \mathrm{N}(0, \sigma^2\varepsilon) & \text{under } H_0 \\ \mathrm{N}(\varepsilon, \sigma^2\varepsilon) & \text{under } H_1 \end{cases}, \tag{2.7}$$

which means that the actual shape of the impulse response does not affect the probabilities of detection and false alarm. The matched filter is not optimal in the Neyman-Pearson sense if the interference is not zero mean white Gaussian noise, but can still be said to maximise the SNR at its output [44]. In essence, the matched filter simply correlates its impulse response with the input signal. If the SOI is present and it is aligned with the impulse response, the output should be maximum. To determine an optimal threshold γ_0' in the Neyman-Pearson sense, the inverse CDF method can be used as demonstrated in the earlier examples.

The detector can be modified so that the cross-correlation coefficient between the filter's impulse response and the input signal is used as the test statistic. This is achieved by dividing the output of the matched filter by a

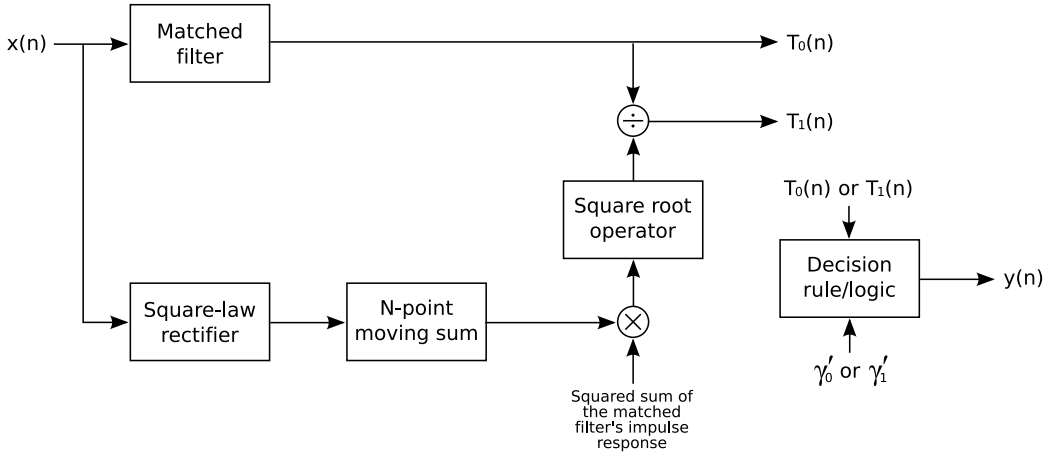

Figure 2.5: Block diagram of a detector that can be used to detect the presence of a known waveform. The design uses a matched filter whose output $T_0(n)$ should be maximum when the SOI is present. The output of the matched filter can be modified so that the cross-correlation coefficient $T_1(n)$ between the input signal and the matched filter's impulse response is computed instead. Now the decision threshold can be chosen in a more intuitive way by defining the relative similarity that is required for detection.

suitable normalisation factor, as depicted in the block diagram of Figure 2.5. Now, the test is given by

$$T_1(n) = \frac{T_0(n)}{\sqrt{\varepsilon \cdot \sum_{k=0}^{N-1} x^2(n-k)}} > \gamma_1'.$$

The value of the cross-correlation coefficient always lies on the interval $[-1, 1]$. Hence, the threshold γ_1' can be chosen in an intuitive way by defining the relative similarity that is required for detection. But then again, the probabilities of detection and false alarm are more difficult to determine. The difficulty comes from the fact that the test statistic is a ratio of two correlated random variables from different distribution families. At least under H_0 an asymptotic distribution can be found for the modified test statistic. Under H_0, the normalisation factor can be written as

$$\sqrt{\varepsilon \cdot \sum_{k=0}^{N-1} w^2(n-k)} = \sqrt{\varepsilon N \cdot \frac{1}{N} \sum_{k=0}^{N-1} w^2(n-k)} = \sqrt{\varepsilon N \hat{\sigma^2}},$$

where $\hat{\sigma^2}$ is an unbiased estimator of σ^2.[4] Now, as $N \to \infty$, or in an asymptotic sense,

$$T_1(n) \to \frac{T_0(n)}{\sqrt{\varepsilon N \sigma^2}} \quad \text{under } H_0.$$

It follows that

$$T_1(n) \overset{\text{a}}{\sim} \mathrm{N}\big(0, \tfrac{1}{N}\big) \quad \text{under } H_0.^{5}$$

This result has been illustrated in Figure 2.6 for $N = 51$. The PDF estimate was obtained with Monte Carlo simulations and the histogram method. A histogram of the simulation results was computed and its values scaled so that reasonable CDF estimates could be obtained with the Riemann sum method when equal subinterval lengths were assumed. Because the test statistic's asymptotic PDF does not depend on the noise variance under H_0, the modified matched filter detector can be said to be asymptotically a CFAR detector.

The detector gives an indication of detection only once for each detected occurrence of the SOI. New detections are impossible until the test statistic falls again below the threshold. The local maximum between the threshold crossings is used to estimate the location of the SOI. The initial location is corrected for the delay of $(N-1)/2$ samples that is induced by the matched filter section. The first $N-1$ values of the test statistic are zeroed in order to suppress premature detections.

An application example is shown in Figure 2.7. The task was to detect QRS complexes from an electrocardiogram (ECG). A QRS complex is a prominent wave shape of the heart cycle that is caused by the rapid depolarisation of the ventricles. The duration between successive QRS complexes, known as the R-R interval, can be used to compute an estimate of the instantaneous heart rate. The ECG signal was measured with a sampling frequency of 500 Hz and a passband of 0.07–192 Hz. The measured signal was pre-processed with an infinite impulse response (IIR) high-pass filter, having the Z-transform

$$H(z) = \frac{1 - z^{-1}}{1 - 0.995 z^{-1}},$$

[4]The unbiasedness of $\hat{\sigma^2}$ comes from

$$\mathrm{E}\big(\hat{\sigma^2}\big) = \frac{1}{N}\sum_{k=0}^{N-1} \mathrm{E}\big(w^2(k)\big) = \frac{1}{N}\sum_{k=0}^{N-1} \Big(\underbrace{\mathrm{E}\big(w^2(k)\big) - \underbrace{\mu^2}_{0}}_{\sigma^2} \Big) = \frac{1}{N} \cdot N \cdot \sigma^2 = \sigma^2.$$

[5]Symbol "$\overset{\text{a}}{\sim}$" denotes "is asymptotically distributed according to".

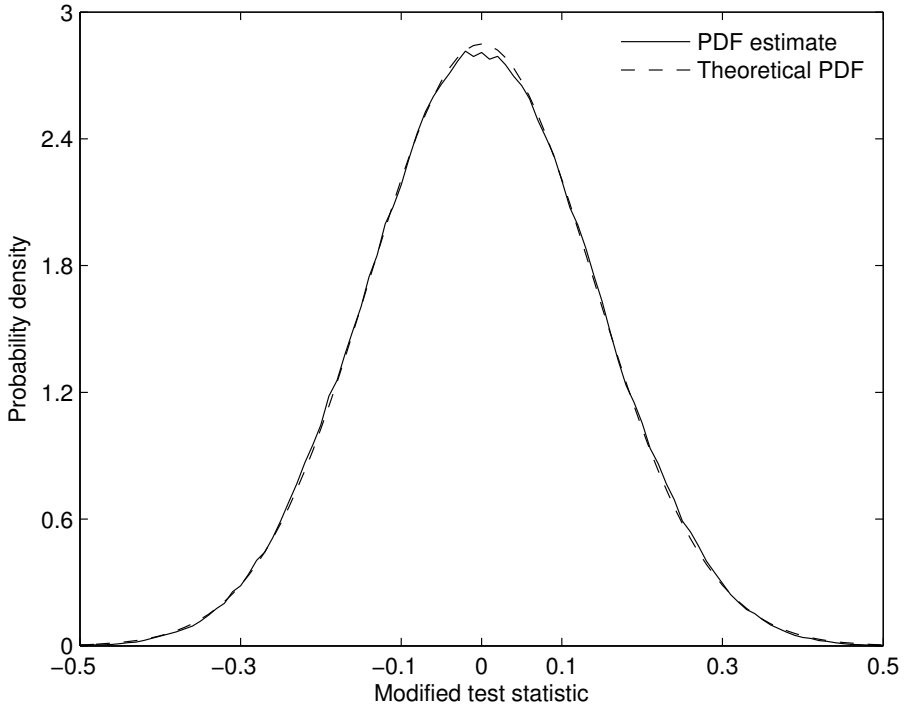

Figure 2.6: Experimental PDF estimate and theoretical asymptotic PDF of the modified test statistic of the matched filter detector under H_0. The length of the matched filter's impulse response was 51 samples. The PDF estimate (solid line) was obtained with Monte Carlo simulations and the theoretical asymptotic PDF (dashed line) is the PDF of $\mathrm{N}\big(0, \frac{1}{51}\big)$.

in order to remove baseline drift. The matched filter section of the modified matched filter detector was designed as follows. First, 10 representative QRS complexes were extracted from the ECG signal. Second, the QRS complexes were temporally aligned and a prototype impulse response was computed by averaging across the QRS complexes. Finally, the prototype impulse response was reversed to acquire the matched filter's impulse response. The matched filter had 51 coefficients. The threshold $\gamma_1' = 0.5$ was used because it accommodates for a moderate correlation. The first 50 values of the test statistic were zeroed in order to prevent premature detections. Laplacian noise was used in order to simulate interfering noise spikes (location and scale parameters 0 and $\sqrt{0.5}$, respectively, and amplified by a factor of 50). In addition, this set-up shows that the detector can operate even though the Gaussian noise assumption is not entirely valid. ■

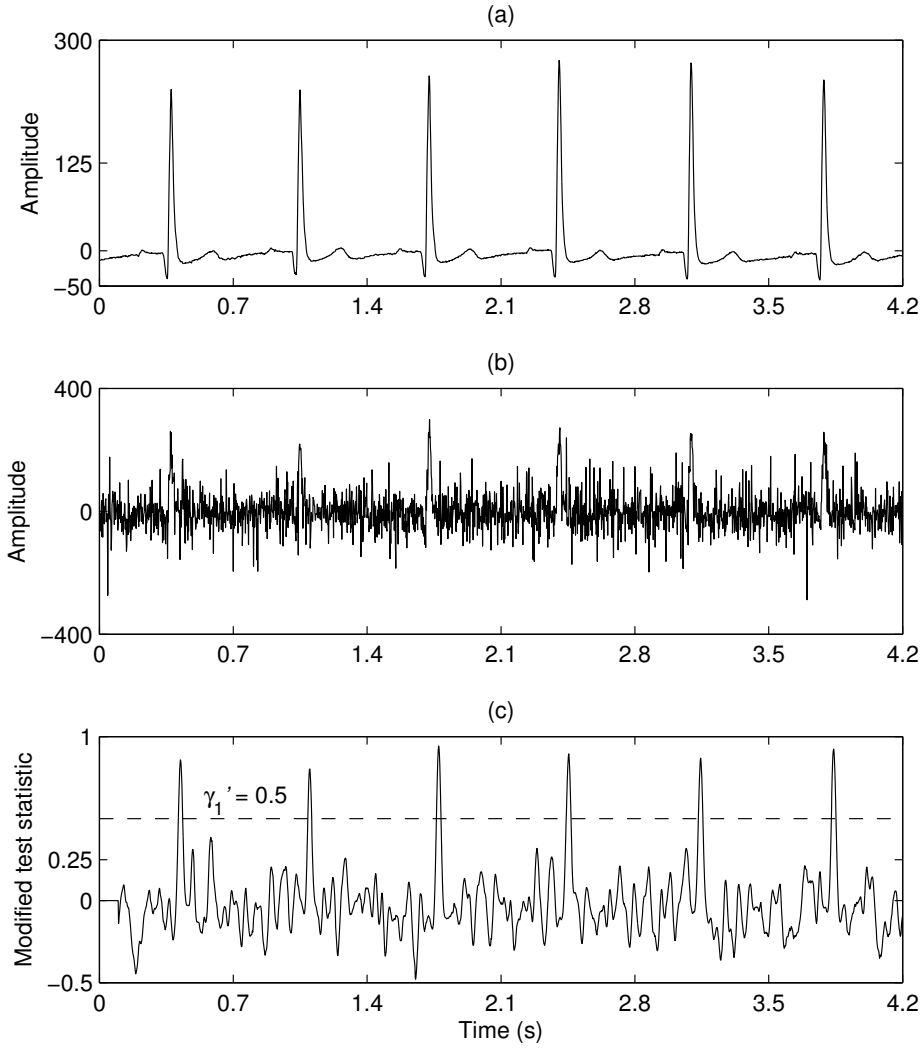

Figure 2.7: Example of using the detector of Figure 2.5 to detect QRS complexes from an ECG signal (a) embedded in Laplacian noise (b). The test statistic (c) gives the cross-correlation coefficient, which is close to unity when a QRS complex is present. The dashed horizontal line represents a threshold that accommodates for a moderate correlation.

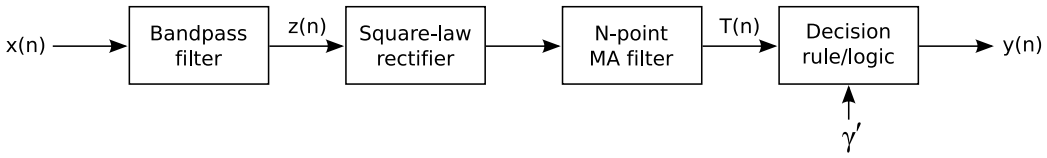

Figure 2.8: Block diagram of a detector that can be used to detect a narrow band signal, such as a sinusoid of a given frequency. The band-pass filter passes the frequency band of interest. Then an estimate of the signal variance is computed with a cascade of a square-law rectifier and an MA filter. The SOI is said to be present if the variance estimate is sufficiently larger than a fixed threshold.

Example 5 – Energy detection

This example considers the application of the energy detector to a detection problem where the SOI is a sinusoid of a known frequency. The energy detector is portrayed as a block diagram in Figure 2.8. The band-pass filter passes the frequency band of interest and the following cascade of a square-law rectifier and an N-point MA filter computes an estimate of the signal variance. Kay [44] does not incorporate a band-pass filter into the energy detector, but we will follow Green and Swets [31] who make such incorporation. This makes sense because in our example the SOI is a sinusoid of a known frequency. The band-pass filter is a narrowband filter whose centre frequency f_c (Hz) matches the frequency of the sinusoid to be detected and whose coefficients are normalised so that the maximum amplification in the passband is 0 dB. The energy detector implements the test

$$T(n) = \frac{1}{N}\sum_{k=0}^{N-1} z^2(n-k) > \gamma', \tag{2.8}$$

where $z(n)$ is the output of the band-pass filter. Let

$$z(n) = \begin{cases} w(n) & \text{under } H_0 \\ s(n) + w(n) & \text{under } H_1 \end{cases},$$

where the noise samples $w(n)$ are IID, follow $\mathrm{N}(0, {\sigma_\mathrm{n}}^2)$, and ${\sigma_\mathrm{n}}^2$, the noise variance after band-pass filtering, is positive. According to (2.7), ${\sigma_\mathrm{n}}^2 = \sigma^2\varepsilon$, where σ^2 is the noise variance before band-pass filtering and ε is the squared sum of the band-pass filter's impulse response. One should not be confused although the detector is called an energy detector but the test statistic is an estimator of the average signal power. This issue can be rectified simply by multiplying the test statistic by N. Green and Swets [31] present PDFs of the

test statistic under both hypotheses, but they assumed an ideal band-pass frequency response and did not consider the correlation induced by discrete-time filtering. Indeed, the consecutive output samples of a practical finite impulse response (FIR) filter are correlated. Furthermore, as the length of the filter's impulse response increases, so does the time span of the correlation. For example, if the correlation issue is disregarded, it follows from (2.5) that

$$T(n) \sim \Gamma\big(\tfrac{N}{2}, \tfrac{2{\sigma_{\mathrm{n}}}^2}{N}\big) \quad \text{under } H_0.$$

This is not the case in practice, however, as illustrated in Figure 2.9. The band-pass filter was a 51-point linear phase FIR filter whose centre frequency and the half-power bandwidth were, approximately, 5 and 3.5 Hz, respectively. The length of the MA filter was 21 samples. The PDF estimate was obtained in the same way as in Example 4. If the band-pass filter is ignored and the input signal scaled to achieve the noise variance of ${\sigma_{\mathrm{n}}}^2$, the two PDFs will coincide. Hence, the difference is caused mainly by the correlation induced by the FIR band-pass filter.

Although the inter-sample correlation makes it difficult to derive the PDFs of the test statistic, there are other ways to determine feasible values for the various detector parameters. For example, we can expand the test statistic given in (2.8) under both hypotheses:

$$T(n) = \frac{1}{N}\sum_{k=0}^{N-1} z^2(n-k) = \frac{1}{N}\sum_{k=0}^{N-1} w^2(n-k) = \hat{{\sigma_{\mathrm{n}}}^2} \quad \text{under } H_0$$

and

$$\begin{aligned} T(n) &= \frac{1}{N}\sum_{k=0}^{N-1} z^2(n-k) = \frac{1}{N}\sum_{k=0}^{N-1} \big(s(n-k)+w(n-k)\big)^2 \\ &= \frac{1}{N}\sum_{k=0}^{N-1} \big(s^2(n-k) + 2s(n-k)w(n-k) + w^2(n-k)\big) \\ &= \frac{1}{N}\sum_{k=0}^{N-1} s^2(n-k) + \frac{2}{N}\sum_{k=0}^{N-1} s(n-k)w(n-k) + \frac{1}{N}\sum_{k=0}^{N-1} w^2(n-k) \\ &= \hat{\varphi} + \frac{2}{N}\sum_{k=0}^{N-1} s(n-k)w(n-k) + \hat{{\sigma_{\mathrm{n}}}^2} \quad \text{under } H_1, \end{aligned}$$

where $\hat{{\sigma_{\mathrm{n}}}^2}$ is an unbiased estimator of ${\sigma_{\mathrm{n}}}^2$ and $\hat{\varphi}$ is an unbiased estimator of

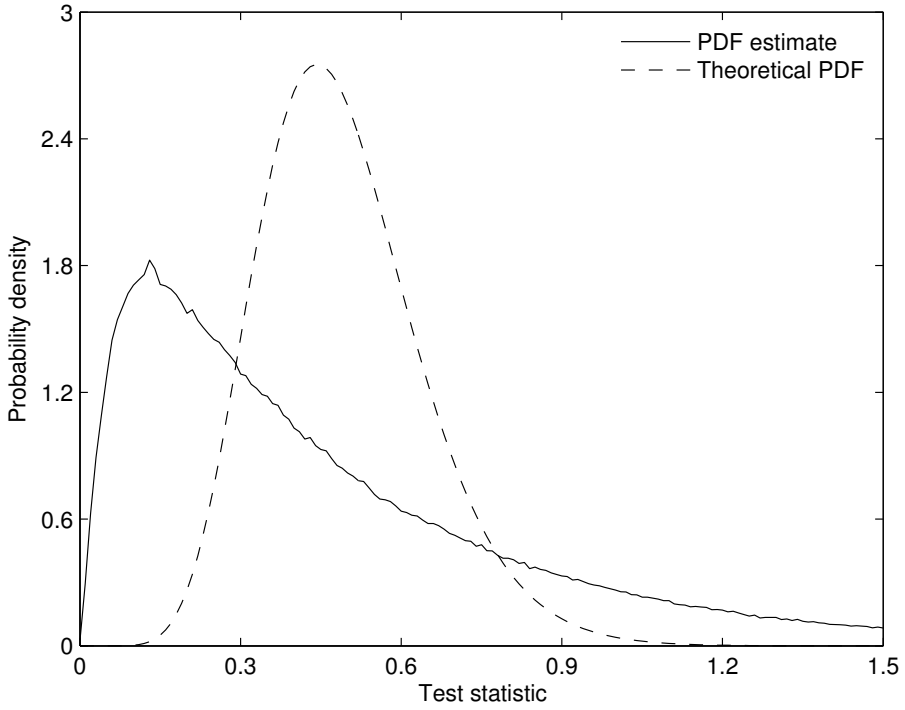

Figure 2.9: Experimental PDF estimate and theoretical PDF of the test statistic $T(n)$ of an exemplar energy detector under H_0. The PDF estimate (solid line) was obtained with Monte Carlo simulations. The theoretical PDF (dashed line) is the PDF of $\Gamma\big(\frac{21}{2}, \frac{2{\sigma_{\mathrm{n}}}^2}{21}\big)$. If the band-pass filter is ignored and the input signal scaled to achieve the noise variance of ${\sigma_{\mathrm{n}}}^2$, the two PDFs will coincide.

$\varphi = A^2/2$, the mean-square value of a sinusoid of amplitude A.[6] Furthermore,

$$\mathrm{E}\big(T(n)\big) = \mathrm{E}\big(\hat{\sigma_{\mathrm{n}}}^2\big) = {\sigma_{\mathrm{n}}}^2 \quad \text{under } H_0$$

[6]The unbiasedness of $\hat{\varphi}$ comes from

$$\mathrm{E}\big(\hat{\varphi}\big) = \frac{1}{N}\sum_{k=0}^{N-1} \underbrace{\mathrm{E}\big(s^2(n-k)\big)}_{\text{mean of } A^2\sin^2(x)} = \frac{1}{N}\cdot N \cdot \frac{A^2}{2\pi}\underbrace{\int_0^{2\pi} \sin^2(x)\,dx}_{\pi} = \frac{A^2}{2}.$$

and

$$\mathrm{E}\big(T(n)\big) = \mathrm{E}\big(\hat{\varphi}\big) + \frac{2}{N} \cdot \underbrace{\mathrm{E}\left(\sum_{k=0}^{N-1} s(n-k)w(n-k)\right)}_{0} + \mathrm{E}\big(\hat{\sigma_{\mathrm{n}}^2}\big)$$

$$= \frac{A^2}{2} + {\sigma_{\mathrm{n}}}^2 \quad \text{under } H_1.$$

With these we can define at least in some sense sensible bounds for the threshold γ'. For example, an intuitive approach would be to choose the threshold so that

$$\frac{A^2}{2} + {\sigma_{\mathrm{n}}}^2 > \gamma' > {\sigma_{\mathrm{n}}}^2. \tag{2.9}$$

If we do not have better knowledge of σ^2, we could choose

$$\gamma' = \frac{A^2/2}{2}. \tag{2.10}$$

A reasonable value for N is given by

$$\left\lceil \frac{F_{\mathrm{s}}}{f_{\mathrm{c}}} + 1 \right\rceil,$$

where $F_{\mathrm{s}}/f_{\mathrm{c}}$ gives the duration of one cycle of a sinusoid of frequency f_{c} in samples. An additional sample is added because every $(F_{\mathrm{s}}/f_{\mathrm{c}})$th sample can be seen common between adjacent cycles. Ceiling function guarantees that the resulting value is an integer.

An application example is shown in Figure 2.10. The task was to detect the presence of a 5 Hz sinusoid, whose amplitude was 2, embedded in zero mean white Gaussian noise. The sampling frequency was 100 Hz. The band-pass filter was a linear phase FIR filter of type 1. It was designed with the window method using the Kaiser window (window parameter was 0.5). Specifications stated that the lower and upper cutoff frequencies should be 3 and 7 Hz, respectively. The designed filter had 51 coefficients and its centre frequency and the half-power bandwidth were, approximately, 5 and 3.5 Hz, respectively. The length of the MA filter was 21 samples. The detector reports that the SOI is present if the test statistic is larger than $\gamma' = 1$, which was chosen according to (2.10). The first 70 values of the test statistic were zeroed in order to guarantee full immersion on part of both filters. Even though the sinusoid is embedded in a relatively strong noise, the detector is able to indicate regions where it is present. However, the delay of 35 samples (350 ms) that is induced by the cascaded filter sections could be seen as a moderate weakness. ■

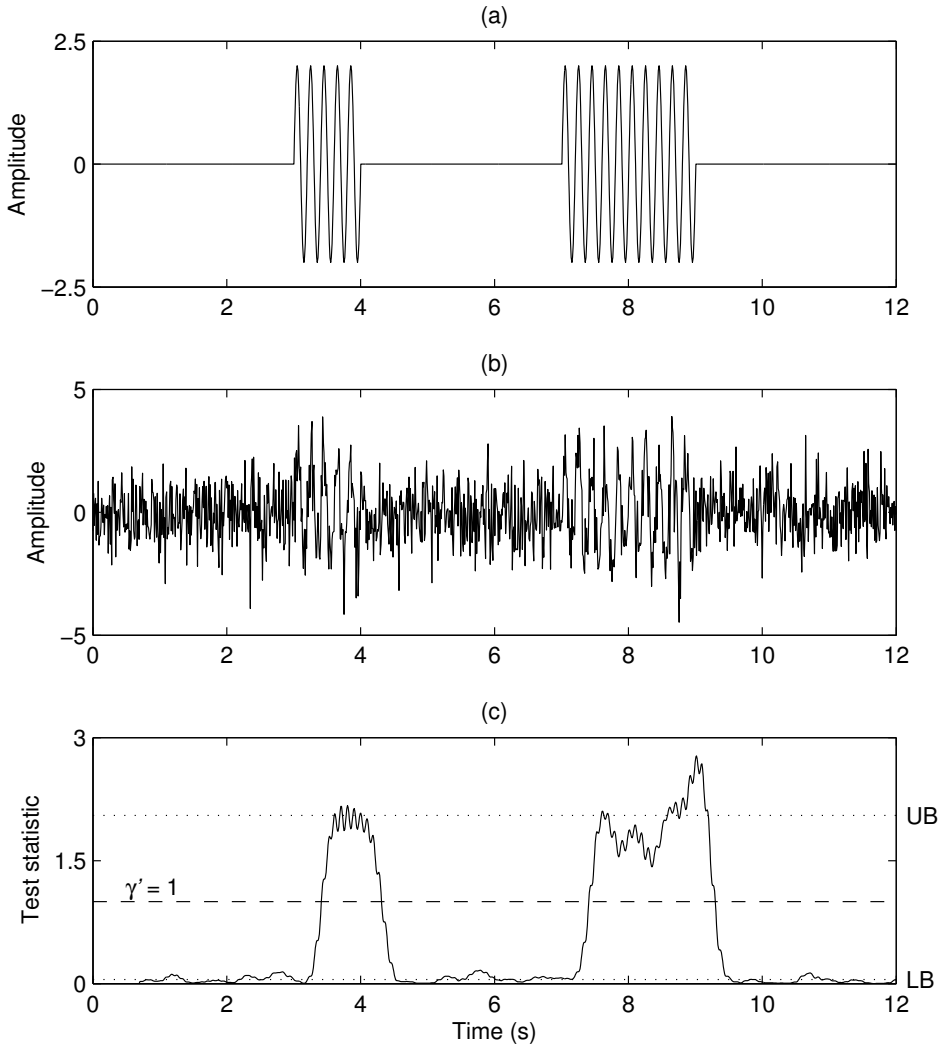

Figure 2.10: Example of using an energy detector to detect the presence of a 5 Hz sinusoid (a) embedded in white Gaussian noise (b). The test statistic (c) gives an estimate of the signal power. The horizontal dotted lines represent upper (UB) and lower (LB) bounds according to (2.9). The horizontal dashed line represents a threshold computed with (2.10).

2.3 Performance evaluation

The probabilities of detection and false alarm are usually of interest when the performance of a detector is discussed. The probability of detection describes how well the presence of the SOI is detected by the detector, whereas the probability of false alarm describes how susceptible the detector is to the effects of noise. According to Section 2.1, both probabilities can be expressed in terms of the test statistic's PDFs under corresponding hypotheses. In addition to the detection criteria, such as the threshold, both probabilities are also functions of certain detector and noise parameters. Because of the common zero mean white Gaussian noise assumption, the noise is usually characterised simply by its variance. Where the probability of false alarm is a function of the above-mentioned parameters, the probability of detection is also a function of certain SOI related parameters.[7] Because both probabilities are computed by integrating the test statistic's PDF under certain hypothesis, as in (2.3) and (2.4), we have to know them in order to compute both probabilities. If we are unable to derive the exact PDFs, then sometimes we can at least come up with asymptotic PDFs, as in Example 4. It should be noted that the traditional definitions of the two probabilities consider only a single threshold as the decision criterion. Indeed, it may happen that although we were able to find the PDFs of the test statistic, they could not be used in a straightforward manner to compute the (overall) probabilities of detection and false alarm.

If we are unable to analytically derive even the asymptotic PDFs of the test statistic, the only option is to revert to the experimental approach in performance evaluation. An obvious course of action is to experimentally derive the PDFs of the test statistic under both hypotheses. This calls for Monte Carlo simulations where we use repeated random sampling to acquire data that is used to derive estimates of the PDFs. The problem with Monte Carlo simulations is that if we wish to get accurate estimates, we have to repeat the simulations a considerable number of times. In addition, if we want to achieve as general results as with the analytical approach, the same set of simulations have to be repeated for numerous parameter combinations, which yields a family of PDF estimates. In other words, the derivation of the test statistic's PDFs may become a very laborious task if the experimental approach is used. The PDFs can be estimated, for example, by using the histogram method, which was used in Examples 4 and 5, or by fitting some known distribution to the data. Density estimation in general, and other

[7] However, as hinted in Example 3, the probability of false alarm does not depend on the noise variance in case of a CFAR detector.

specific approaches besides the above two, are discussed in the literature [10, 23, 84].

Because of the aforementioned problems, or maybe because the objective is merely to demonstrate the function of a detector in certain circumstances, the detector may be tested in a restricted set-up and PDF estimation ignored altogether. In such set-up, the test data is processed with the detector under evaluation and the results are analysed by computing suitable performance measures. Because we do not know the PDFs of the test statistic, the probabilities of detection and false alarm cannot be used. Alternative measures are the true alarm rate (TAR) and the false alarm rate (FAR) given by

$$\frac{N_\mathrm{d}}{N_\mathrm{s}} \quad \text{and} \quad \frac{N_\mathrm{fa}}{N_\mathrm{r}},$$

respectively, where N_d is the number of correct detections, N_s is the number of occurrences of the SOI, N_fa is the number of false detections, and N_r is the number of all reported detections. These quantities conform to the following restrictions:

$$N_\mathrm{d} \leq N_\mathrm{s}, \quad N_\mathrm{fa} \geq 0, \quad N_\mathrm{r} = N_\mathrm{d} + N_\mathrm{fa} \geq N_\mathrm{s}, \quad \text{and} \quad N_\mathrm{s} > 0.$$

Which detection is defined to be correct, or a true alarm, depends on the actual test set-up. The TAR is the proportion of correctly detected occurrences of the SOI, whereas P_d is the probability that the test statistic is larger than the threshold when the SOI is present. Hence, the TAR may be seen as an estimate of P_d as $N_\mathrm{s} \to \infty$. The same cannot be said about FAR and P_fa. Where the FAR is the proportion of false detections out of all reported detections, P_fa is the probability that the test statistic is larger than the threshold when only noise is present. In other words, N_fa is compared with N_r and not with all time instants the test statistic could have been above the threshold. A modified measure N_fa/L, where L is the number of time instants when the SOI is absent, could be used to estimate P_fa, however. In addition, one should not be mistaken to think that FAR has something to do with CFAR. If a detector has the CFAR property, the detector tries to maintain constant P_fa, not constant FAR although the appellation CFAR would suggest otherwise.

When using the experimental approach in performance evaluation, either genuine or artificial data is required to perform the necessary experiments. Using artificial data relates to the setting where we assume to have full knowledge of the input signal's distributions under both hypotheses. Indeed, with artificial data we have full control over the noise parameters, the interfering artefacts, the occurrences of the SOI and its parameters, etc. Simply put,

the whole test set-up is under absolute control. If genuine data is used, then some of these are out of the control of the experimenter. For example, with artificial data, the exact locations of the occurrences of the SOI are known, whereas with genuine data they are not. If these were identified by a human expert, then subjective criteria would certainly affect the results. Besides, an average human observer cannot easily process vast amounts of numerical data because of boredom and fatigue. Indeed, artificial data provides objectiveness that cannot be guaranteed with genuine data. Even so, one can always argue that the results obtained with artificial data cannot fully represent those obtained in realistic situations. Because of this, genuine data should be used to verify the function of a detector in a realistic situation. In addition, genuine data can also reveal certain not well-defined concepts such as distinction between false and nuisance alarms as discussed in Section 4.2 of Publication II.

The aforementioned performance measures do not tell how good or accurate the detections are. Some additional measures are required to answer such questions. Particularly, the accuracy of the SOI related parameter estimates, the temporal accuracy of detection, and the latency of detection have to be assessed. If the detector is used in a near real-time application, also computational complexity [19] of a detector should be of interest. It should be noted, however, that low computational complexity alone does not guarantee suitability for a near real-time application. Low computational complexity merely suggests that all computations required by a single time step may possibly be carried out during one sampling interval. Also the latency of detection, which can usually be controlled by adjusting the detector parameters, determines if the detector is suitable for a near real-time application. In the end, however, each practical discrete-time system induces some time delay.

Chapter 3

Selected Contributions

This thesis is based on studies presented in five articles that can be classified into two subcategories according to the detection problem they address. These are the detection of muscle contractions and the detection of saccadic eye movements. In this chapter, the relevant biomedical signals and the associated detection problems are introduced and short descriptions of the five articles are given.

3.1 Detection of muscle contractions

The function of muscles is to generate force and motion. They enable locomotion and tend to various vital bodily functions. There are three types of muscle tissue: skeletal, smooth, and cardiac. Skeletal muscles are anchored to bones by tendons and generate the movements of the endoskeleton and the body. Smooth muscles generate the movements of internal organs. For example, the (thoracic) diaphragm has an important role as part of the respiratory system as it is responsible for the ventilation of the lungs. As another example, the musculature of the digestive tract produces peristalsis that propels food and enables digestion. Cardiac muscle tissue can only be found in the heart. The heart is the central unit of the circulatory system whose function results in the circulation and distribution of blood, oxygen, and nutrients in the body. Smooth muscles and the cardiac muscle are controlled by the autonomic nervous system. Only skeletal muscles can be controlled voluntarily. Muscles under voluntary control are of greater importance in this thesis. Therefore, the structure and function of only skeletal muscle tissue will be considered in detail.

The function of muscles is enabled by their capability to contract. Contraction capability, in turn, comes from the structure and the electrochemical

properties of the muscle tissue [14, 69, 88]. A muscle is composed of numerous muscle fibres whose diameters are orders of magnitude smaller than a millimetre. Muscle fibres are made up of smaller structures known as myofibrils. Myofibrils, in turn, are mainly composed of actin and myosin based protein filaments that are organised into repeated sub-units, called sarcomeres, along the length of the myofibril so that they can slide in an interlocking manner. The interlocking of the protein filaments causes the shortening of the myofibril and, consequently, the shortening of the whole muscle fibre. When this happens, the muscle fibre is said to undergo a contraction. Muscles are divided into functional units referred to as motor units. A motor unit, which is the smallest muscle unit that can be activated by volitional effort [69], is composed of a motor neurone, its axon, and all muscle fibres innervated by the axon. Motor neurones are primarily located in the anterior horn of the spinal cord, but in the case of the head muscles they are located in the cranial nerves of the brain stem [14]. When a motor neurone is activated, its action potential travels along the axon towards the muscle tissue where the neurotransmitter acetylcholine is released into the innervated muscle fibres. This initiates electrochemical reactions that cause the contraction of the muscle fibres. The contraction of a muscle is the consequence of the contraction of its muscle fibres.

Electromyography is concerned with the measurement, processing, and analysis of electrical signals originating from the muscle tissue. The function of a motor unit generates an electrical signal referred to as the motor unit action potential. The superposition of the action potentials of all active motor units is the basis of the electromyographic (EMG) signal, or the electromyogram, which can be measured with instruments ranging from invasive fine-wire and needle electrodes to non-invasive surface electrodes of various shapes and sizes. The location of the studied muscle and the scope of the investigation govern the choice of the measurement instruments [70]. In medicine EMG signals are used in the diagnosis of neuromuscular diseases, disorders of muscle functions, and chronic pain [17, 52, 67, 69]. In psychophysiology EMG signals have been used to investigate affective influences [50]. In addition, novel human-machine interaction techniques based on EMG signals have been investigated in tasks such as controlling a traditional computer [7, 18, 39, 65, 81], a wheelchair [27], and an artificial prosthesis [2, 24, 35, 71, 64, 66, 79].

Because invasive techniques may be painful to the subject and there is a risk of inflammation and damage when the muscle tissue is penetrated, EMG signals are typically measured with non-invasive bipolar surface electrodes. The resulting signal is referred to as the surface EMG signal. It is common to use an alternating current (AC) powered differential amplifier. Most energy

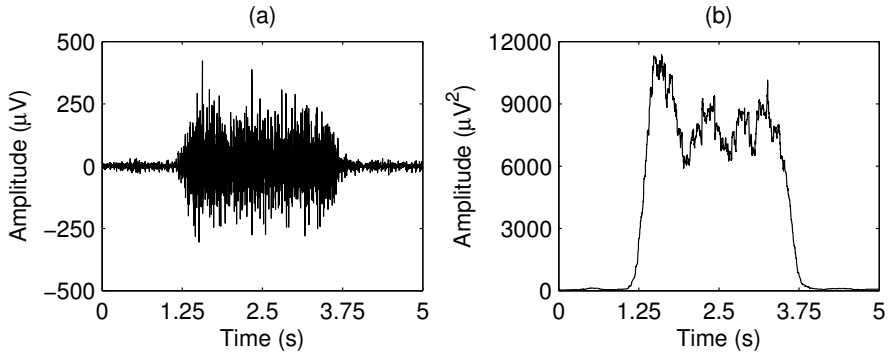

Figure 3.1: Segment of facial surface EMG signal (a) measured with bipolar surface electrodes and an AC powered differential amplifier. The waveform in (b) gives an estimate of the instantaneous variance. An onset and a termination of muscle contraction occur, approximately, at 1.25 s and 3.75 s, respectively.

in a bipolar measured surface EMG signal resides between 10 and 200 Hz. Therefore, the measurement passband is chosen so that this frequency band is preserved. A typical passband ranges from 10 to 500 Hz, although applied passbands vary to some extent [14, 16, 21, 28, 88]. A narrower passband is used in order to attenuate excessive interference that is caused, for example, by baseline wandering, movement artefacts, signals from other physiological sources, power-line noise, and high frequency noise. A surface EMG signal presents a stochastic nature in its samples, as illustrated in Figure 3.1. The moving average remains close to zero, because of the band-pass filtering, whereas the instantaneous variance fluctuates with the level of muscle contraction. The signal is seldom used in its raw form but processed in some meaningful way to acquire a more suitable presentation. The instantaneous variance is just one possible approach. The reader is referred to [51] for an investigation on different quantification techniques.

The detection of muscle contractions is usually done before carrying out further analysis. As it was suggested above, the onset and the termination of muscle contraction are embodied as changes in the instantaneous variance of a surface EMG signal. Hence, from the viewpoint of detection theory, we are dealing with a model change detection problem. Several computer-based methods have been developed for the detection of the onset of muscle contraction. Notable comparisons between various methods have been conducted by Hodges and Bui [36] and Staude et al. [80]. However, these investigations were limited to the single-trial onset detection problem and neither termination detection nor performing detections repeatedly were considered.

The capability of detecting both the onset and the termination of muscle contraction repeatedly is essential in near real-time applications. Two different approaches to solving the described detection problem are considered in Publications I and II.

3.1.1 Neural network based detector (I)

A multi-layer perceptron (MLP) neural network was used as the core component of the detector in Publication I. An artificial neural network, or simply neural network, is a distributed parallel processing system capable of learning its operation from the input data [10, 23, 33, 34, 82, 84].[1] A neural network is composed of neurones that are connected to each other with weighted connections. A single neurone is a relatively simple element and is capable of computing only a simple function of its input, but a network of neurones is capable of computing far more complex functions. The neurones of an MLP are organised into two or more layers (see Figure 3.2). The neurones of the input layer perform no computations and their sole purpose is to relay the input to the following layers. An MLP may contain a number of hidden layers whose neurones perform computations. So do the neurones of the final layer, the output layer, whose output also makes up the overall output of the MLP. The MLP is a feedforward neural network because the information flows in one direction, from the input layer towards the output layer. There are no feedback connections.

The objective of the study was to develop and test an MLP-based detector that can be used to detect voluntarily produced contractions of corrugator supercilii and zygomaticus major facial muscles. A block diagram of the detector is shown in Figure 3.3. Either band-pass filtering or wavelet denoising [55] is used for pre-processing. Normalised root-mean-square (RMS) values computed from the adjacent sub-segments of the observed signal segment make up the input of the MLP. RMS was used because according to LeVeau and Andersson [51] it is a good descriptor of the EMG signal in a mathematical sense. The MLP classifies the signal segment into one of the three classes representing the onset of muscle contraction, the termination of muscle contraction, and constant level of muscle contraction. The tested MLPs had two input neurones, from zero to five hidden neurones in one layer or five neurones in two hidden layers each, and three output neurones corre-

[1] The research on artificial neural networks has been motivated from the beginning by the fact that the human brain processes data in an entirely different way than a conventional computer does [33]. Indeed, the human brain has been the paragon for neural networks. Neural network attempts to mimic some properties of its biological counterpart, such as non-linearity, generalisation, fault tolerance, and learning capability.

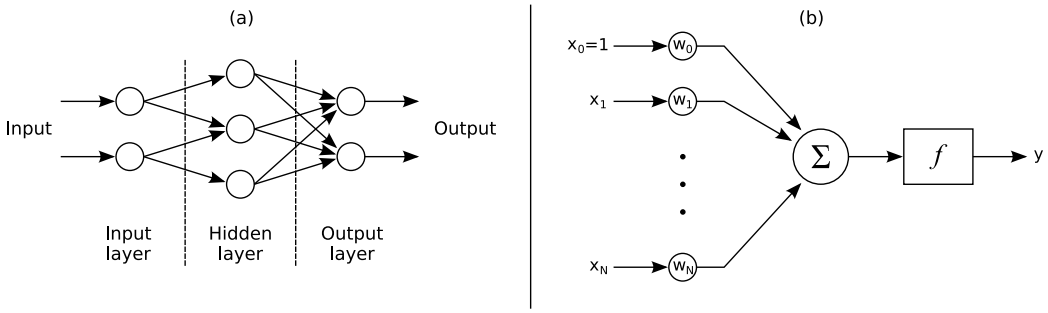

Figure 3.2: Exemplar MLP neural network (a). The network has 2 input, 3 hidden, and 2 output neurones organised into respective layers. The MLP is a feedforward neural network because the information flows in one direction, as indicated by the arrows. Only the hidden and the output neurones perform computations. Such a neurone (b) computes a function of the weighted sum of its inputs, where the weights $w_0, \ldots, w_N$ correspond to the inputs $x_0, \ldots, x_N$. The function f is known as the activation function of the neurone. It is typically a sigmoidal function such as the logistic function $f(x) = \frac{1}{1+\exp(-ax)}$, where a controls the slope of the function.

sponding to the three output classes. The results show that the MLP-based detector functions well, producing recognition accuracies ranging from 96 to 99%. The best accuracies were achieved with one hidden layer of two to five neurones after wavelet denoising. Also the smallest MLP without any hidden neurones functioned well. Because all tested MLPs were small in respect to the number of computational neurones, the computational requirements of the detector should not be an issue.

Although the results suggest that the MLP-based detector enjoys the generalisation property of neural networks, this is probably caused by the use of normalised RMS values: the normalised RMS values do not carry on the information about the absolute magnitude of the observed EMG signal. Also, the good performance of the smallest MLP supports this claim: the output neurones alone are capable of solving the underlying classification problem. Furthermore, if one considers the performance of the MLP with one hidden neurone, the input data from the two input neurones are compressed into one value that is enough for the output neurones to form a mapping to the three output classes. There is one considerable drawback in applying the MLP-based detector. If the detector is operated in a sequential manner in order to perform detections repeatedly, the output values of the MLP will saturate at some point, which complicates the estimation of the onset and termination locations. The saturation is caused by the sigmoidal activation

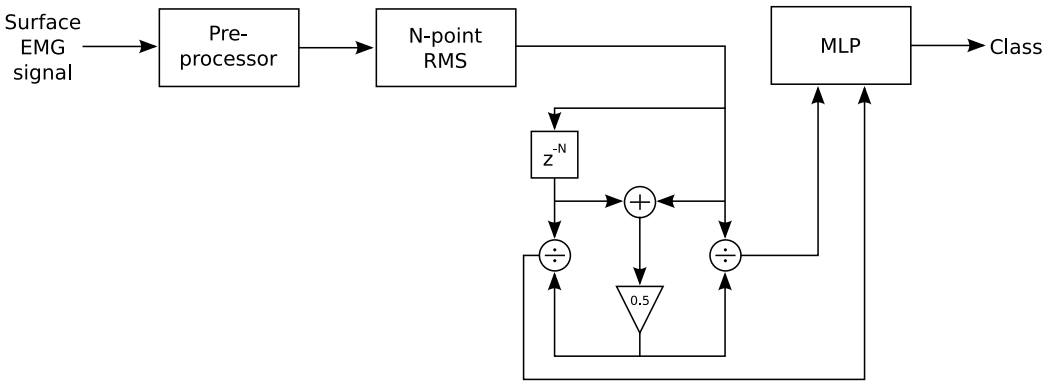

Figure 3.3: Block diagram of the MLP-based detector. The pre-processor is either a traditional band-pass filter or a wavelet denoiser. Normalised RMS values computed from the adjacent sub-segments of the observed signal segment make up the input of the MLP. The output of the MLP reflects the classification of the observed signal segment.

functions. The fact that the MLP has to be trained can also be seen as another drawback of the MLP-based detector. In other words, a considerable amount of preliminary work is required before the MLP-based detector can be put into practical use. The considered detection problem may be too simple to justify the use of a neural network. The task of classifying limb movements on the basis of an EMG signal offers a more suitable application area. See, for example, [63, 64, 66, 79].

3.1.2 Modified two-point backward difference (II)

The motivation behind the detector of Publication II was that it can be used without training and it does not suffer from similar saturation issues as the MLP-based detector. A block diagram portraying the detector is shown in Figure 3.4. The surface EMG signal is first pre-processed with a band-pass filter in order to reduce the disturbing effects of interference. The pre-processed signal is input to an envelope detector that extracts the modulating envelope waveform. On the basis of this waveform, a modified two-point backward difference (MTPBD) is used to compute a test statistic that reflects the occurrence of either an onset or a termination of muscle contraction. The decision logic takes care of both the decision making and the estimation of event locations. The described detector can be implemented in a computationally efficient manner with conventional DSP techniques. Therefore, it can be used in near real-time applications. The results that were obtained experimentally on artificial data show that the MTPBD detector functions

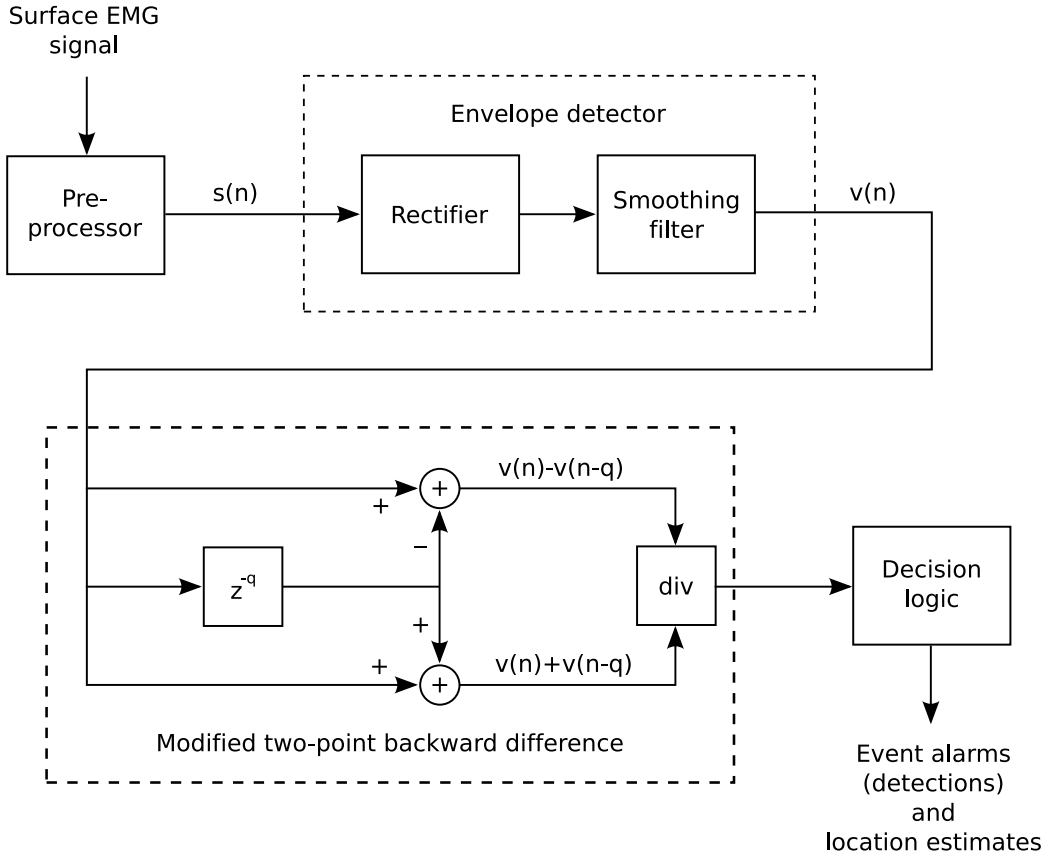

Figure 3.4: Block diagram of the MTPBD detector. $s(n)$ is the pre-processed surface EMG signal, $v(n)$ is the extracted envelope waveform, and $v(n-q)$ is its delayed version.

reliably if a long enough MA filter is used for smoothing in the envelope detector. Verification that was conducted with a few genuine surface EMG signals supports the obtained results. Afterwards, a detector configuration using RMS values in place of the envelope detected samples was tested. The results were virtually identical with those obtained with an envelope detector using a square-law rectifier.

Although the MTPBD adds to the non-linearity of the detector and, therefore, complicates its analytical analysis, the choice of the detection threshold can be made on a relative basis. Thus, the detector can be easily used with signals originating from different subjects. Also, if the detector is operated by a non-technically oriented person, this can be seen as a clear advantage. For a technically oriented person, the MTPBD detector does not appear simply as a black box system, which can be the case with the MLP-

based detector. Guidelines for choosing the detector parameters were given. Also, a detailed description of the experimental set-up was presented. The set-up includes a signal generator that can be used to generate artificial surface EMG signals. By using the Publication II as a guide, one can implement an identical signal generator.

The MTPBD detector has already been used in an experimental human-computer interface that uses optical gaze tracking and facial surface EMG signals. Voluntary facial muscle contractions were detected in order to emulate mouse clicks. The results from this preliminary investigation were promising and they show that the MTPBD detector can also be used in practice.

3.2 Detection of saccadic eye movements

Eyes are photosensitive sensory organs that make up the front-end of the human visual system. The lens of an eye focuses the light onto the retina. The photoreceptor cells of the retina, which are the rods and cones, convert the light into nerve impulses [56]. The nerve impulses make up the visual information that is transmitted to the brain via the optic nerve. The fovea, an area on the retina where the photoreceptor cells, mainly cones that enable colour vision, are densely packed and the resolution is highest, is small and the eyes have to be moved so that the target of interest would be aligned with this focal area. The capability of fixating on the target of interest in the visual field comes from the musculature of an eye. Six orbital muscles generate horizontal, vertical, and torsional eye movements. Eye movements appear in varying amplitudes and patterns. Movement velocities may reach several hundred degrees per second.

The analysis of eye movements has proven to be valuable in both medical work and research. Eye movement research has been conducted by various authors [4, 5, 25, 29, 86]. In medicine eye movement data are used to investigate and diagnose, for example, vestibular or otoneurological disorders [42, 56], Parkinson's disease [15], optic ataxia [45], and various other conditions [47]. Eye movement data is also used in sleep studies [1, 11, 72]. Besides medical applications, eye movement data has been used in various human-machine interfaces. Example tasks include controlling a traditional computer [12, 13, 30, 38, 43, 48, 54, 58, 81, 83, 90], operating assistive robots and platforms [46, 87], and guiding a wheelchair [6, 68].

Eye movements can be measured with different methods, but optical and electrical are probably the most common ones. In this thesis, we are concerned with the electrical method of measuring eye movements. A pair of

surface electrodes are affixed to the temples of the subject in order to measure horizontal eye movements, whereas vertical eye movements can be measured with a pair of surface electrodes affixed above and below either eye socket. The resulting signals are referred to as electro-oculographic (EOG) signals, or electro-oculograms. The basis of the EOG signal is the standing potential of the eye, which is caused by the potential difference between the cornea and the retina. As the eye rotates, the standing potential measured at the electrodes changes. Both AC and direct current (DC) powered amplifiers can be used in the measurement of EOG signals. Which one to use depends on the objective of the application. If the eye position information is to be preserved, a DC powered amplifier has to be used because with an AC powered amplifier the signal drifts towards zero level after each eye movement. Regardless of the type of the amplifier, the measurement passband may be limited below 50 Hz because it results in the attenuation of both high frequency and power-line noise. However, a higher low-pass cutoff frequency should be used in order to preserve information describing the velocity and acceleration of rapid eye movements. Applied low-pass cutoff frequencies vary considerably. Reported cutoff frequencies include, for example, 5 Hz [90], 10 Hz [46], 35 Hz [1, 5, 6], 40 Hz [86], 42 Hz [91], 70 Hz [15], 75 Hz [83], 100 Hz [54], and "less than 500 Hz" [48].

The detection of saccadic eye movements, or simply saccades, and the extraction of related parameters, such as maximum angular velocity, amplitude, and duration, are usually performed during the analysis of EOG signals. Typically saccades are detected by comparing the rectified velocity waveform of an EOG signal to a fixed threshold. If the threshold is exceeded, a saccade is said to be present. Different techniques such as duration limiting [5, 78], several test statistics and rejection criteria [1], adaptive filters and thresholds [15, 40, 85], and syntactic methods [41, 42] have been used to implement more robust saccade detection methods. As illustrated in Figure 3.5, saccades can be identified as fast jumps in the EOG signal and as prominent peaks and valleys in the velocity waveform. This observation reveals why so many saccade detection methods analyse the velocity waveform in order to detect saccades. If the SNR is relatively high and the noise characteristics are known beforehand and they do not change, a simple detector employing a fixed detection threshold can be used to accomplish the detection task. But if these assumptions do not hold, some form of sensitivity adjustment has to be performed in order to limit the number of false alarms. Publications III and IV introduce two techniques, cell-averaging (CA) and order-statistic (OS) CFAR, for implementing a saccade detector that continuously adjusts its detection sensitivity in order to maintain a constant false alarm probability. The developed detector was refined and subjected to a

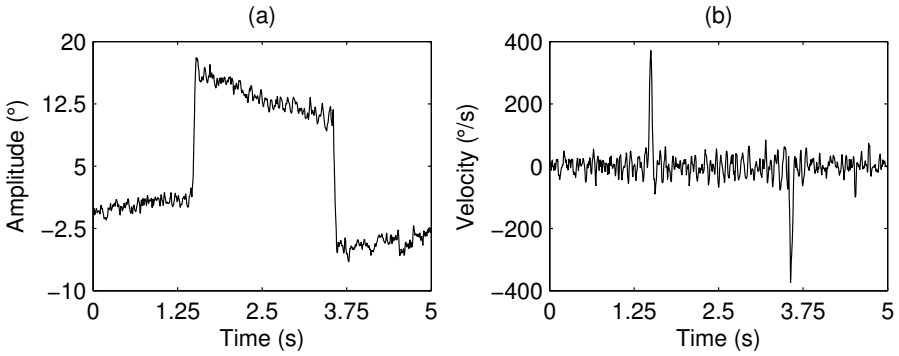

Figure 3.5: Example of a horizontal EOG signal (a), measured with bipolar surface electrodes and an AC powered amplifier, and the corresponding velocity waveform (b). Saccades can be identified in (a) as fast jumps in the signal level and in (b) as prominent peaks and valleys.

more in-depth analysis in Publication V.

3.2.1 Introducing CA and OS CFAR (III & IV)

The main motivation for using CFAR was that optimal measurement conditions cannot be always guaranteed with novel wearable measurement equipment, and an adaptive system could probably operate satisfactorily even if the noise characteristics change during the measurement. The CFAR techniques discussed in Publications III and IV are not new, but they have been used in radar receivers [75, 76]. Actually, another motivation was that the velocity peaks of saccadic eye movements resemble the echoes of simple targets at the output of the demodulator of a radar receiver. Therefore, it was thought that it would not be difficult to adapt the particular techniques to be suitable for detecting saccades from an EOG signal. Both publications show that this was indeed the case.

A block diagram of the CFAR saccade detector is shown in Figure 3.6. Either a low-pass or a band-pass filter is used for pre-processing. The preprocessed EOG signal is input to a two-point central difference differentiator that extracts the velocity waveform. The velocity waveform is full-wave rectified and input to the CFAR processor, where an adaptive threshold is computed by first computing a certain noise statistic and then multiplying it by a constant s, whose value depends on the desired false alarm probability. The statistic is the sample mean in case of CA CFAR and a specific order statistic in case of OS CFAR. The decision logic compares the outputs of the CFAR processor and makes a decision regarding the presence of a saccade

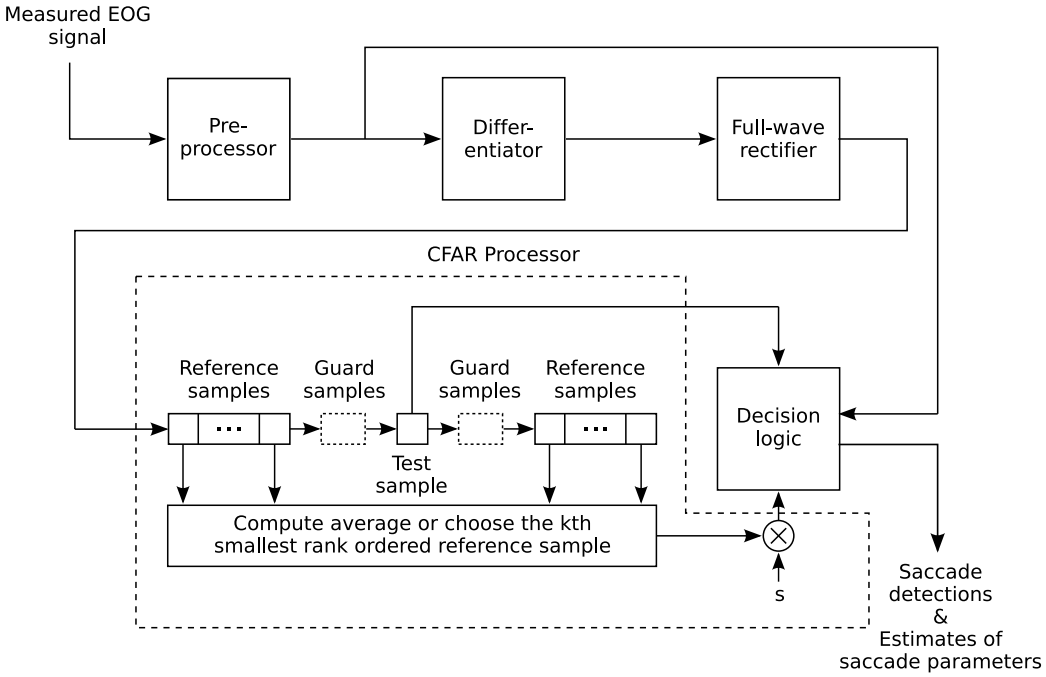

Figure 3.6: Block diagram portraying the architecture of the CFAR saccade detector. The reference samples are used to compute an adaptive threshold. Depending on the type of the CFAR processor, either the average or a specific order statistic is used in the computation of the threshold value. The value of s depends on the desired false alarm probability.

accordingly. The CFAR saccade detector is computationally efficient, it can operate autonomously without user assistance, and it is capable of detecting saccades in a sequential fashion. Closed form expression for estimating the value of the constant s, under zero mean white Gaussian noise assumption, was derived for both CFAR techniques. Other detector parameters received more attention in Publication V.

3.2.2 Experimenting with the CFAR approaches (V)

A refined version of the CFAR saccade detector was presented in Publication V. In contrast to Publications III and IV, the detector was subjected to a more in-depth analysis, which included a comparison against a typical detection method that uses a fixed detection threshold. The results show that both CFAR techniques can be used to decrease the number of false alarm in noisy conditions. Therefore, the CFAR saccade detector finds potential use in applications where fast and automated signal analysis is a requirement,

ideal measurement conditions cannot be guaranteed, and noise presents a considerable problem. Such applications include, for example, the human-machine interfaces that were mentioned earlier in Section 3.2. Because the detector performed well in case of a relatively high SNR, it can also be used in more traditional medical applications. Indeed, although a human expert would verify the analysis results, enforcing low false alarm probability leads into fewer false alarm and, consequently, less verification work. In addition, the application example of Publication V clearly showed that because of the sensitivity adjustment, the CFAR saccade detector can be easily used with EOG signals originating from different subjects without laborious search for suitable parameters.

However, constant false alarm probability is maintained at the expense of the detection sensitivity, which means that some of the smaller saccades are missed. To elaborate, as the detection threshold is increased in order to maintain a low false alarm probability, the probability of detection is decreased. This should not be a surprise after recalling Section 2.1. The decrease in detection sensitivity has to be tolerated when using a CFAR detector and, particularly, if the desired false alarm probability is low. Also, one should understand that a CFAR technique does not guarantee false alarm free operation: the appellation CFAR stands for constant false alarm probability, not zero false alarm probability. It should be also noted that the CFAR property holds only if the true noise distribution resembles the assumed noise distribution. If one would have to choose between CA and OS CFAR, it would be rather difficult on the basis of the obtained results because both performed equally well. However, if the number of reference samples is small, OS CFAR may be a better choice. Particularly, order statistics near the median are not as sensitive to outliers as the mean is.

In the end, maybe the best approach would be a hybrid system that incorporates the best of both worlds: rely on a fixed detection threshold until the noise characteristics change in such a way that it is beneficial to use an adaptive threshold. The decision logic could be improved by using some SOI related parameters to suppress false alarms. Indeed, if the decision logic were more sophisticated, the desired false alarm probability could be higher. The design of an optimal differentiator was not considered. If the differentiator were better, in other words, it attenuated noise as well as possible but at the same time preserved the velocity waveform during saccades, the overall performance might be improved. Incorporating even some of the ideas could be a step closer towards a better saccade detector.

The problem of choosing various detector parameters received more attention than in Publications III and IV. While certain parameters can be computed with closed form equations, others have to be chosen intuitively.

The number of reference and guard samples serve as examples. However, experimental knowledge, such as the amplitude-duration relationship, can be used to alleviate the situation. Also, a detailed description of the experimental set-up was presented. The set-up includes a signal generator that can be used to generate artificial EOG signals. By using the Publication V as a guide, one can implement an identical signal generator.

Chapter 4

Discussion

This thesis considered the detection of muscle contractions and saccadic eye movements on the basis of biomedical signals originating from facial landmarks. While participating in two successive projects aimed at developing novel human-computer interaction techniques, the author of the thesis designed, implemented, and tested practical detectors that can be used to detect the aforementioned physiological events. The main design goals were the capability of operating in the presence of noise, the capability of adapting to changes in the noise characteristics, the capability of processing signals originating from different subjects without laborious search for suitable parameters, and low computational requirements, which is essential if a detector is used in a near real-time application such as a human-computer interface. Although human-computer interaction gave the basic motivation for the research, there is no reason why the developed detectors could not be used in more traditional medical applications, such as research work, medical diagnosis, and patient monitoring.

Publications I and II focused on the problem of detecting the onset and the termination of muscle contraction on the basis of a surface EMG signal. The MLP approach was considered in Publication I. The results show that the MLP-based detector is functional. Even the smallest MLP with least computational power functioned surprisingly well. Therefore, computational requirements should not be an issue. There are, however, some drawbacks in the MLP approach. Particularly, the output values of the MLP will saturate at some point if the detector is operated in a sequential manner, which complicates the estimation of the onset and termination locations. The fact that the MLP has to be trained can be also seen as a weakness. The amount of preliminary work can be reduced by using the detector of Publication II. The results show that the MTPBD detector functions reliably if a long enough MA filter is used for smoothing in the envelope detector. The MTPBD detec-

tor is computationally efficient and it does not suffer from similar saturation issues as the MLP-based detector. Therefore, the estimation of the onset and termination locations is easier. Because the choice of the detection threshold can be made on a relative basis, the MTPBD detector can be easily used with signals originating from different subjects. Also, if the detector is operated by a non-technically oriented person, this can be seen as a clear advantage. Finally, because surface EMG signals originating from different muscles are similar, both detectors can be also used in applications that do not focus on facial muscles.

Publications III–V focused on the detection of saccadic eye movements from an EOG signal with a CFAR detector. The main motivation for choosing CFAR was that optimal measurement conditions cannot be always guaranteed with novel wearable measurement equipment, and an adaptive system could probably operate satisfactorily even if the noise characteristics change during the measurement. The CFAR techniques considered are not new, but they have been used in both radar and sonar receivers. Actually, another motivation was that the velocity peaks of saccadic eye movements resemble the echoes of simple targets in a radar signal. The work and the results presented in Publications III–V show that the particular CFAR techniques could be adapted to another field and they offer a method for lowering the number of false alarms in noisy conditions. Therefore, the CFAR saccade detector finds potential use in applications where fast and automated signal analysis is a requirement, ideal measurement conditions cannot be guaranteed, and noise presents a considerable problem. However, constant false alarm probability is maintained at the expense of the detection sensitivity, which means that some of the smaller saccades are missed. This has to be tolerated when using a CFAR detector and, particularly, if the desired false alarm probability is low.

The five publications illustrated some of the problems that are present when designing and testing detectors. First of all, there is not necessarily a common set of genuine test data available. Therefore, comparing detectors is usually difficult or laborious. For example, the results of Publication I represent only one set of test data. Using some other data would probably had yielded different results. In addition, although it is commonly recognised that genuine data represent the ultimate test for any system, genuine data do not necessarily provide as much control or objectiveness as artificial data. These issues were also discussed in Section 2.3. Because of the aforementioned issues, artificial data were used in the experiments of Publications II and V. Still, genuine data were used to verify the results. One problem of detector design is the choice of suitable parameters. Sometimes detectors are designed and tested with some set of parameters, but no guidelines, even

intuitive ones, are presented for choosing them. In Publications II–V, we tried to present such guidelines. These guidelines are useful when a detector is applied in practice.

The software components used to conduct the experiments were at first implemented in Matlab code. As the research work progressed, all detectors and necessary components, excluding the MLP-based detector, were implemented in C++. Because the various components are implemented as classes, they can be easily used in other C++ programs. This facilitates and speeds up the ensuing software development process because the detectors have already been implemented.

Near future endeavours include further development of the saccade detector considered in Publications III–V. One of the objectives is to integrate it into the "Face Interface", which was presented in Chapter 1, as it would enable the analysis of saccadic eye movements. Baseline drift poses a notable problem in an EOG signal measured with a DC powered amplifier. Another objective is to use the CFAR saccade detector in a novel drift removal system. While participating in the second project, the author of the thesis has been developing a frowning detector that operates on a signal measured with a capacitive sensor. The future work shows if this approach is better, or worse, than the surface EMG approach used in Publication II.

Personal Contributions

I (the author of the thesis) and Martti Juhola designed the experimental set-up of Publication I. I conducted the experiments and analysed the results with Martti Juhola. The article was mostly written by Martti Juhola and Veikko Surakka while I wrote some parts of it. On the part of Publications II–IV, I designed the experimental set-ups, conducted the experiments, analysed the results, and wrote the articles, while Martti Juhola provided guidance. Publication V is my own work.

Bibliography

[1] R. Agarwal, T. Takeuchi, S. Laroche, and J. Gotman. Detection of rapid-eye movements in sleep studies. *IEEE Transactions on Biomedical Engineering*, Vol. 52, No. 8, 2005, pp. 1390–1396.

[2] K. Akazawa, R. Okuno, and M. Yoshida. Biomimetic EMG prosthesis-hand. *Proceedings of EMBC'96* (Amsterdam, The Netherlands, 1996), pp. 535–536.

[3] U. Appel and A.V. Brandt. A comparative study of three sequential time series segmentation algorithms. *Signal Processing*, Vol. 6, No. 1, 1984, pp. 45–60.

[4] A.T. Bahill, A. Brockenbrough, and B.T. Troost. Variability and development of a normative data base for saccadic eye movements. *Investigative Ophthalmology*, Vol. 21, No. 1, 1981, pp. 116–125.

[5] R.W. Baloh, A.W. Sills, and W.E. Kumley. Quantitative measurement of saccade amplitude, duration, and velocity. *Neurology*, Vol. 25, No. 11, 1975, pp. 1065–1070.

[6] R. Barea, L. Boquete, M. Mazo, and E. López. System for assisted mobility using eye movements based on electrooculography. *IEEE Transactions on Neural Systems and Rehabilitation Engineering*, Vol. 10, No. 4, 2002, pp. 209–218.

[7] A.B. Barreto, S.D. Scargle, and M. Adjouadi. A practical EMG-based human-computer interface for users with motor disabilities. *Journal of Rehabilitation Research and Development*, Vol. 37, No. 1, 2000, pp. 53–64.

[8] M. Basseville and I.V. Nikiforov. *Detection of Abrupt Changes: Theory and Application*. Prentice-Hall, Inc., Englewood Cliffs, NJ, US, 1993.

[9] T. Bayes. An essay towards solving a problem in the doctrine of changes. *Philosophical Transactions of The Royal Society of London*, Vol. 53, 1763, pp. 370–418. Available at http://www.stat.ucla.edu/history/essay.pdf (accessed 1 June 2009).

[10] C.M. Bishop. *Neural Networks for Pattern Recognition*. Oxford University Press, Oxford, UK, 1995.

[11] S. Boyer and V. Kapur. Role of portable sleep studies for diagnosis of obstructive sleep apnea. *Current Opinion in Pulmonary Medicine*, Vol. 9, 2003, pp. 465–470.

[12] A. Bulling, D. Roggen, and G. Tröster. It's in your eyes – towards context-awareness and mobile HCI using wearable EOG goggles. *Proceedings of UbiComp'08* (Seoul, Korea, 2008), pp. 84–93.

[13] A. Bulling, D. Roggen, and G. Tröster. Wearable EOG goggles: eye-based interaction in everyday environments. *Proceedings of CHI'09* (Boston, MA, US, 2009), pp. 3259–3264.

[14] J.T. Cacioppo, L.G. Tassinary, and G. Berntson. *Handbook of Psychophysiology, 2nd Edition*. Cambridge University Press, Cambridge, UK, 2000.

[15] T. Chen, Y.-F. Cyhen, C.-H. Lin, and T.-T. Tsai. Quantification analysis of saccadic eye movements. *Annals of Biomedical Engineering*, Vol. 26, 1998, pp. 1065–1071.

[16] E.A. Clancy, E.L Morin, and R. Merletti. Sampling, noise-reduction and amplitude estimation issues in surface electromyography. *Journal of Electromyography and Kinesiology*, Vol. 12, 2002, pp. 1–16.

[17] A. Cohen. *Biomedical Signal Processing*. CRC Press, Inc., Boca Raton, FL, US, 1986.

[18] K. Coleman. Electromyography based human-computer-interface to induce movement in elderly persons with movement impairments. *Proceedings of the 2001 EC/NSF Workshop on Universal Accessibility of Ubiquitous Computing: Providing for the Elderly* (Alcácer do Sal, Portugal, 2001), pp. 75−79.

[19] T.H. Cormen, C.E. Leiserson, R.L. Rivest, and C. Stein. *Introduction to Algorithms, 2nd Edition*. The MIT Press, Cambridge, MA, US, 2001.

[20] R.L. Dawe. *Detection Threshold Modelling Explained.* Aeronautical and Maritime Research Laboratory, Defence Science and Technology Organisation (DSTO), Melbourne, Victoria, Australia, 1997.

[21] C.J. De Luca. *Surface Electromyography: Detection and Recording.* Delsys, 2002. Available at http://www.delsys.com/Attachments_pdf/WP_SEMGintro.pdf (accessed 1 June 2009).

[22] P.S.R. Diniz, E.A.B. da Silva, and S.L. Netto. *Digital Signal Processing: System Analysis and Design.* Cambridge University Press, Cambridge, UK, 2002.

[23] R.O. Duda, P.E. Hart, and D.G. Stork. *Pattern Classification, 2nd Edition.* John Wiley & Sons, Inc., New York, NY, US, 2001.

[24] V. Dunfield and E. Shwedyk. Digital E.M.G. processor. *Medical & Biological Engineering & Computing*, Vol. 16, 1978, pp. 745–751.

[25] C.J. Erkelens. Coordination of smooth pursuit and saccades. *Vision Research*, Vol. 46, 2006, pp. 163–170.

[26] Face Interface. Project website available at https://www.cs.uta.fi/∼wtpc/?q=node/7 (accessed 1 June 2009).

[27] T. Felzer and B. Freisleben. HaWCoS: the 'hands-free' wheelchair control system. *Proceedings of ASSETS'02* (Edinburgh, Scotland, UK, 2002), pp. 127–134.

[28] A.J. Fridlund and J.T. Cacioppo. Guidelines for human electromyographic research. *Psychophysiology*, Vol. 23, 1986, pp. 567–589.

[29] S. Garbutt, M.R. Harwood, and C.M. Harris. Infant saccades are not slow. *Developmental Medicine & Child Neurology*, Vol. 48, 2006, pp. 662–667.

[30] J. Gips and P. Olivieri. EagleEyes: An eye control system for persons with disabilities. *Proceedings of the 11th International Conference on Technology and Persons with Disabilities* (Los Angeles, CA, US, 1996).

[31] D.M. Green and J.A. Swets. *Signal Detection Theory and Psychophysics.* John Wiley & Sons, Inc., New York, NY, US, 1966.

[32] A.V. Halteren, R. Bults, K. Wac, D. Konstantas, I. Widya, N. Dokovsky, G. Koprinkov, V. Jones, and R. Herzog. Mobile patient monitoring: the MobiHealth system. *The Journal on Information Technology in Healthcare*, Vol. 2, No. 5, 2004, pp. 365–373.

[33] S. Haykin. *Neural Networks – A Comprehensive Foundation, 2nd Edition*. Prentice-Hall, Inc., Upper Saddle River, NJ, US, 1999.

[34] R. Hecht-Nielsen. *Neurocomputing*. Addison-Wesley Publishing Company, Inc., Reading, MA, US, 1990.

[35] A. Herrera, A. Bernal, D. Isaza, and M. Adjouabi. Design of an electrical prosthesis gripper using EMG and linear motion approach. *Proceedings of FCRAR'04* (Orlando, FL, US, 2004).

[36] P.W. Hodges and B.H. Bui. A comparison of computer-based methods for the determination of onset of muscle contraction using electromyography. *Electroencephalography and Clinical Neurophysiology*, Vol. 101, 1996, pp. 551-519.

[37] E.C. Ifeachor and B.W. Jervis. *Digital Signal Processing: A Practical Approach, 2nd Edition*. Prentice-Hall, Inc., 2001.

[38] R.J.K. Jacob. The use of eye movements in human-computer interaction techniques: what you look at is what you get. *ACM Transactions in Information Systems*, Vol. 9, No. 3, 1991, pp. 152–169.

[39] H. Jeong, J.-S. Kim, and J.-S. Choi. A study of an EMG-controlled HCI methods by clenching teeth. *Proceedings of APCHI'04* (Rotorua, New Zealand, 2004), 163–170.

[40] M. Juhola, V. Jäntti, I. Pyykkö, M. Magnusson, L. Schalén, and M. Åkesson. Detection of saccadic eye movements using a non-recursive adaptive digital filter. *Computer Methods and Programs in Biomedicine*, Vol. 21, 1985, pp. 81–88.

[41] M. Juhola. A syntactic method for analysis of saccadic eye movements. *Pattern Recognition*, Vol. 19, 1986, pp. 353–359.

[42] M. Juhola, H. Aalto, and T. Hirvonen. Using results of eye movement signal analysis in the neural network recognition of otoneurological disorders. *Computer Methods and Programs in Biomedicine*, Vol. 86, 2007, pp. 216–226.

[43] A.E. Kaufman, A. Bandopadhay, and B.D. Shaviv. An eye tracking computer user interface. *Proceedings of VR'93* (San Jose, CA, US, 1993), pp. 120–121.

[44] S.M. Kay. *Fundamentals of Statistical Signal Processing (Volume 2): Detection Theory*. Prentice-Hall PTR, Upper Saddle River, NJ, US, 1998.

[45] A.Z. Khan, J.D. Crawford, G.B.C. Urquizar, and Y. Rossetti, and L. Pisella. Influence of initial hand and target position on reach errors in optic ataxic and normal subjects. *Journal of Vision*, Vol. 7, No. 5, 2007, pp. 1–16.

[46] Y. Kim, N. Doh, Y. Youm, and W.K. Chung. Development of human-mobile communication system using electrooculogram signals. *Proceedings of the 2001 IEEE/RSJ International Conference on Intelligent Robots and Systems* (Maui, HI, US, 2001), pp. 2160–2165.

[47] A.E. Krill. The electroretinogram and electro-oculogram: clinical applications. *Investigative Ophthalmology*, Vol. 9, No. 8, 1970, pp. 600–617.

[48] D. Kumar and E. Poole. Classification of EOG for human computer interface. *Proceedings of the Second Joint EMBS/BMES Conference* (Houston, TX, US, 2002), pp. 64–67.

[49] C. Kunze, U. Großmann, W. Stork, and K.D. Müller-Glaser. Application of ubiquitous computing in personal health monitoring systems. *Proceedings of BMT'02* (Berlin, Germany, 2002), pp. 360–362.

[50] J.T. Larsen, C.J. Norris, and J.T. Cacioppo. Effects of positive and negative affect on electromyographic activity over zygomaticus major and corrugator supercilii. *Psychophysiology*, Vol. 40, 2003, pp. 776–785.

[51] B. LeVeau and G.B.J. Andersson. Output forms: data analysis and applications – interpretation of electromyographic signals. *Selected Topics in Surface Electromyography for Use in the Occupational Setting: Expert Perspectives*. US Department of Health and Human Services, NIOSH Pub. No. 91–100, March 1992.

[52] P. Lisiński. Surface EMG in chronic back pain. *European Spine Journal*, Vol. 9, 2000, pp. 559–562.

[53] A. Luoma. Personal communication. 28 November 2008.

[54] Z. Lv, X. Wu, M. Li, and C. Zhang. Implementation of the EOG-based human computer interface system. *Proceedings of ICBBE'08* (Shanghai, China, 2008), pp. 2188–2191.

[55] S. Mallat. *A Wavelet Tour of Signal Processing, 2nd Edition*. Academic Press, San Diego, CA, US, 1999.

[56] J. Malmivuo and R. Plonsey. *Bioelectromagnetism – Principles and Applications of Bioelectric and Biomagnetic Fields*. Oxford University Press, New York, NY, US, 1995.

[57] J.I. Marcum. A statistical theory of target detection by pulsed radar. *IRE Transactions on Information Theory*, Vol. 6, No. 2, 1960, pp. 59–267.

[58] J.R. Millán. Adaptive brain interfaces. *Communications of the ACM*. Vol. 46, No. 3, March 2003, pp. 75–80.

[59] S.K. Mitra. *Digital Signal Processing: A Computer-Based Approach, 3rd Edition*. McGraw-Hill, New York, NY, US, 2006.

[60] J. Neyman and E.S. Pearson. On the problem of the most efficient tests of statistical hypotheses. *Philosophical Transactions of the Royal Society of London*, Vol. 231, 1933, pp. 289–337. Available at http://www.jstor.org/pss/91247 (accessed 1 June 2009).

[61] H. Nyquist. Certain topics in telegraph transmission theory. *Transactions of the American Institute of Electrical Engineers*, Vol. 47, 1928, pp. 617–644. Reprinted in *Proceedings of the IEEE*, Vol. 90, No. 2, 2002, pp. 280–305.

[62] A.V. Oppenheim and R.W. Schafer. *Digital Signal Processing*. Prentice-Hall, Inc., Upper Saddle River, NJ, US, 1975.

[63] M.A. Oskoei and H. Hu. Myoelectric control systems – A survey. *Biomedical Signal Processing and Control*, Vol. 2, 2007, pp. 275–294.

[64] P. Parker, K. Englehart, and B. Hudgins. Myoelectric signal processing for control of powered limb prostheses. *Journal of Electromyography and Kinesiology*, Vol. 16, 2006, pp. 541–548.

[65] T. Partala, A. Aula, and V. Surakka. Combined voluntary gaze direction and facial muscle activity as a new pointing technique. *Proceedings of IFIP INTERACT'01* (Tokyo, Japan, 2001), pp. 100–107.

[66] P. Prociow, A. Wolczowski, T.G. Amaral, O.P. Dias, and J. Filipe. Identification of hand movements based on MMG and EMG signals. *Proceedings of BIOSIGNALS'08* (Funchal, Madeira, Portugal, 2008), pp. 534–539.

[67] S.L. Pullman, D.S. Goodin, A.I. Marquinez, S. Tabbal, and M. Rubin. Clinical utility of surface EMG – report of the Therapeutics and Technology Assessment Subcommittee of the American Academy of Neurology. *Neurology*, Vol. 55, 2000, pp. 171–177.

[68] A. Rajan, R.G. Shivakeshavan, and V.R. Jayaraman. Electrooculogram based instrumentation and control system (IC system) and its applications for severely paralysed patients. *Proceedings of the International Conference on Biomedical and Pharmaceutical Engineering* (Singapore, 2006), pp. 1–4.

[69] R.M. Rangayyan. *Biomedical Signal Analysis: A Case-Study Approach.* John-Wiley & Sons, Inc., New York, NY, US, 2002.

[70] G. Rau, E. Schulte, and C. Disselhorst-Klug. From cell to movement: to what answers does EMG really contribute? *Journal of Electromyography and Kinesiology*, Vol. 14, 2002, pp. 611–617.

[71] M. Reischl, R. Mikut, C. Pylatiuk, and S. Schulz. Control strategies for hand prosthesis using myoelectric patterns. *Proceedings of the 9th Fuzzy Colloquium* (Zittau, Germany, 2001), pp. 168–174.

[72] A. Saastamoinen, E. Huupponen, A. Värri, J. Hasan, and S.-L. Himanen. Computer program for automated sleep depth estimation. *Computer Methods and Programs in Biomedicine*, Vol. 82, 2006, pp. 58–66.

[73] M. Schwaibold, M. Gmelin, G. von Wagner, J. Schöchlin and A. Bolz. Key factors for personal health monitoring and diagnosis devices. *Proceedings of Mobile Computing in Medicine 2002* (Heidelberg, Germany, 2002), pp. 143–150.

[74] C.E. Shannon. Communication in the presence of noise. *Proceedings of the Institute of Radio Engineers*, Vol. 37, No. 1, 1949, pp. 10–21. Reprinted in *Proceedings of the IEEE*, Vol. 86, No. 2, 1998, pp. 447–457.

[75] M.I. Skolnik (editor in chief). *Radar Handbook, 2nd Edition.* McGraw-Hill, New York, NY, US, 1990.

[76] M.I. Skolnik. *Introduction to Radar Systems, 3rd Edition.* McGraw-Hill, New York, NY, US, 2001.

[77] S.W. Smith. *The Scientist and Engineer's Guide to Digital Signal Processing, 2nd Edition.* California Technical Publishing, San Diego, CA, US, 1999.

[78] A.T. Smith, P.R.M. Bittencourt, D.S.L. Lloyd, and A. Richens. An efficient technique for determining characteristics of saccadic eye movements using a mini computer. *Journal of Biomedical Engineering*, Vol. 3, 1981, pp. 39–43.

[79] A. Soares, A. Andrade, E. Lamounier, and R. Carrijo. The development of a virtual myoelectric prosthesis controlled by an EMG pattern recognition system based on neural networks. *Journal of Intelligent Information Systems*, Vol. 21, No. 2, 2003, pp. 127–141.

[80] G. Staude, C. Flachenecker, M. Daumer, and W. Wolf. Onset detection in surface electromyographic signals: a systematic comparison of methods. *EURASIP Journal on Applied Signal Processing*, Vol. 2001, Issue 2, 2001, pp. 67–81.

[81] V. Surakka, M. Illi, and P. Isokoski. Gazing and frowning as a new human-computer interaction technique. *ACM Transactions on Applied Perception*, Vol. 1, No. 1, 2004, pp. 40–56.

[82] K. Swingler. *Applying Neural Networks – A Practical Guide.* Academic Press Limited, London, UK, 1996.

[83] J.J. Tecce, J. Gips, C.P. Olivieri, L.J. Pok, and M.R. Consiglio. Eye movement control of computer functions. *International Journal of Psychophysiology*, Vol. 29, 1998, pp. 319–325.

[84] S. Theodoridis and K. Koutroumbas. *Pattern Recognition, 3rd Edition.* Academic Press, San Diego, CA, US, 2006.

[85] J.R. Tole and L.R. Young. Digital filters for saccade and fixation detection. In D.F. Fisher, R.A. Monty, and J.W. Sender (Eds.), *Eye Movements: Cognition and Visual Perception.* Lawrence Erlbaum Associates, Hillsdale, NJ, US, 1981.

[86] M. Versino, G. Castelnovo, R. Bergamaschi, A. Romani, G. Beltrami, D. Zambarbieri, and V. Cosi. Quantitative evaluation of saccadic and smooth pursuit eye movements. *Investigative Ophthalmology & Visual Science*, Vol. 34, No. 5, 1993, pp. 1702–1709.

[87] W.S. Wijesoma, K.S. Wee, O.C. Wee, A.P. Balasuriya, K.T. San, and L.K. Soon. EOG based control of mobile assistive platforms for the severely disabled. *Proceedings of the 2005 IEEE International Conference on Robotics and Biomimetics* (Hong Kong SAR / Macau SAR, China, 2005), pp. 490–493.

[88] D.A. Winter. *Biomechanics of Motor Control of Human Movement, 2nd Edition.* John Wiley & Sons, Inc., New York, NY, US, 1990.

[89] Wireless Technology and Psychophysiological Computing. Project website available at http://www.cs.uta.fi/∼wtpc/wtpc/ (accessed 1 June 2009).

[90] K. Yamagishi, J. Hori, and M. Miyakawa. Development of EOG-based communication system controlled by eight-directional eye movements. *Proceedings of EMBC'06* (New York, NY, US, 2006), pp. 2574–2577.

[91] R.D. Yee, V.L. Schiller, V. Lim, F.G. Baloh, R.W. Baloh, and V. Honrubia. Velocities of vertical saccades with different eye movement recording methods. *Investigative Ophthalmology & Visual Science*, Vol. 26, No. 7, 1985, pp. 938–944.

Addenda and Corrigenda

The following list contains additions clarifying some parts of the text and corrections for errors that were found after the thesis was printed. However, these additions and corrections do not cover Publications I–V but only the introductory part of the thesis.

Page iii, list of keywords.
Add "human-machine interaction" to the end of the list.

Page 1, last complete sentence on page.
Operating room staff was unintentionally omitted from the list. Change the sentence to "Besides physicians performing medical diagnosis, also paramedics, emergency room staff, operating room staff, and intensive care units make considerable use of biomedical signals in patient monitoring."

Page 14, 3rd complete sentence on page.
Change the sentence to "It is usually assumed that if detection occurred in the latter case, then it would certainly occur in the former case as well."

Page 14, 4th to last sentence on page.
Change "moving average" to "moving-average".

Page 19, caption of Figure 2.5.
Add the following sentence before the last sentence: "Divisions by zero can be overcome, for example, by using saturation arithmetic (see Publication II for details)." Also, change the last sentence to: "The threshold γ_1' can be chosen in an intuitive way by defining the relative similarity that is required for detection."

Page 19, 1st complete sentence of the body text.
Add the following sentences, as a footnote, just after the equation defining $T_1(n)$: "This is not the commonly used Pearson correlation coefficient but a normalised version of the cross-correlation. For example, Ifeachor and

Jervis [37] give a similar definition for the cross-correlation coefficient."

Page 19, 2nd to last complete sentence on page.
Change "two correlated random variables" to "two dependent random variables".

Page 23, 1st sentence of the caption of Figure 2.8.
Change "given frequency" to "known frequency".

Page 32, last complete sentence on page.
Change "(AC) powered" to "(AC) coupled".

Page 33, 1st sentence of the caption of Figure 3.1.
Change "AC powered" to "AC coupled".

Page 35, 1st sentence of the 2nd paragraph of the body text.
Replace the colon (:) with a period (.) and begin the following sentence with a capital letter.

Page 36, caption of Figure 3.3.
Add the following sentence before the last sentence: "Divisions by zero can be overcome, for example, by using saturation arithmetic (see Publication II for details)."

Page 36, Section 3.1.2.
No information was given on the tested rectifiers or smoothing filters. Add the following sentences after the 4th sentence of Section 3.1.2: "The envelope detector is a cascade of a rectifier and a smoothing filter. Three types of rectifiers were tested: half-wave, full-wave, and square-law. Only MA smoothing filters were considered. This choice was made because MA filters have linear phase response and they can be implemented in a computationally efficient manner." Also, change the following sentence to "The envelope waveform is input to a modified two-point backward difference (MTPBD) that computes a test statistic reflecting the occurrence of either an onset or a termination of muscle contraction."

Page 37, caption of Figure 3.4.
The role of the delay factor q was not explained. Add the following sentence to the end of the caption: "The delay factor q, whose value mainly depends on the characteristics of the envelope detector, is chosen so that neither $v(n)$ nor $v(n-q)$ is corrupted by information contributing to the other."

Page 39, 4th complete sentence on page.
Change "(DC) powered" to "(DC) coupled".

Page 39, 6th complete sentence on page.
Change "DC powered" to "DC coupled" and "AC powered" to "AC coupled".

Page 40, 1st sentence of the caption of Figure 3.5.
Change "AC powered" to "AC coupled".

Page 41, caption of Figure 3.6.
The role of the guard samples may remain unclear. Add the following sentence before the last sentence: "Information overlap between the test and the reference samples is decreased by placing an appropriate number of guard samples between them."

Page 41, 2nd to last sentence of the 1st paragraph of the body text.
Change "zero mean white Gaussian noise assumption" to "the zero-mean additive white Gaussian noise assumption".

Page 41, last complete sentence on page.
Change "the number of false alarm" to "the number of false alarms".

Page 42, 3rd complete sentence on page.
Change "fewer false alarm" to "fewer false alarms".

Page 49, 1st paragraph.
Add the following sentence to the end of the paragraph: "I designed the detectors considered in the publications."